crystals

MDPI

Review

Effect of LDHs and Other Clays on Polymer Composite in Adsorptive Removal of Contaminants: A Review

Maleshoane Mohapi [1], Jeremia Shale Sefadi [2,*], Mokgaotsa Jonas Mochane [1,*], Sifiso Innocent Magagula [1] and Kgomotso Lebelo [1]

[1] Department of Life Sciences, Central University of Technology, Free State, Private Bag X20539, Bloemfontein 9300, South Africa; shoanymohapi@gmail.com (M.M.); sifisom61@gmail.com (S.I.M.); KLebelo@cut.ac.za (K.L.)

[2] Department of Physical and Earth Sciences, Sol Plaatje University, Kimberley 8301, South Africa

* Correspondence: jeremia.sefadi@spu.ac.za (J.S.S.); mochane.jonas@gmail.com or mmochane@cut.ac.za (M.J.M.)

Received: 15 August 2020; Accepted: 15 October 2020; Published: 22 October 2020

Abstract: Recently, the development of a unique class of layered silicate nanomaterials has attracted considerable interest for treatment of wastewater. Clean water is an essential commodity for healthier life, agriculture and a safe environment at large. Layered double hydroxides (LDHs) and other clay hybrids are emerging as potential nanostructured adsorbents for water purification. These LDH hybrids are referred to as hydrotalcite-based materials or anionic clays and promising multifunctional two-dimensional (2D) nanomaterials. They are used in many applications including photocatalysis, energy storage, nanocomposites, adsorption, diffusion and water purification. The adsorption and diffusion capacities of various toxic contaminants heavy metal ions and dyes on different unmodified and modified LDH-samples are discussed comparatively with other types of nanoclays acting as adsorbents. This review focuses on the preparation methods, comparison of adsorption and diffusion capacities of LDH-hybrids and other nanoclay materials for the treatment of various contaminants such as heavy metal ions and dyes.

Keywords: layered double hydroxides (LDHs); other nanoclays; organically modified LDH; water purification; adsorption; adsorption interaction; diffusion

1. Introduction

A reliable, affordable, sustainable and easily accessible clean water supply chain for many societies in the entire world is an essential component for healthier life and safe environment. However, due to limited economical resources or lack of infrastructure, millions of poor and vulnerable people including children die annually from diseases caused by an inadequate water supply, poor water quality, sanitation and hygiene. Recently, many countries and communities experienced the global challenge/phenomenon known as "Coronavirus (COVID-19) or COV2 infections", which required a frequent washing of hands with clean water and soap or hand sanitizer to avoid or curb the spread (flatten the curve). These key risk aspects or factors adversely impact on food security, livelihood diversities and learning opportunities for poor and most susceptible households across the world. According to the World Health Organization (WHO), almost 1.7 million people lost their lives because of water pollution, and four billion cases of diverse health issues were reported every year due to water borne diseases [1]. Table 1 represents various types of water contaminants, their sources and negative effects. To improve access to quality and safe drinking water, sanitation, and hygiene (WASH), there must be value-added infrastructure investment in dealing with and managing

the freshwater ecosystems and sanitation facilities on a local level in many developing countries. The improved WASH is thus fundamental to poverty reduction, promotion of equality, and support for socioeconomic development under the sustainable development goals (SDGs) [2,3]. The most essential requirements for clean water supply chain is a proper material with high degree of separation capacity, low cost, porosity, and reusability [4–7]. Nanotechnology presents a set of opportunities to develop nanomaterials for effective water purification systems. Optimization of the properties like hydrophilicity, hydrophobicity, porosity, mechanical strength and dispersibility [8–10] is the best option to treat wastewater. Due to their high surface area, high chemical reactivity, adsorption capabilities, excellent mechanical strength and cost-effectiveness, nanomaterials have a huge potential to effectively purify water in numerous ways [8,10–12] by removing various contaminants. This can be done by using different purifiers with different pore sizes such as: microfiltration (MF), ultrafiltration (UF), nanofiltration (NF) and reverse osmosis (RO) (Figure 1). However, the main stumbling block associated with addition of 2D nanomaterials is the aggregation or agglomeration that restricts their effective use in many industrial applications. This daunting aggregation or agglomeration challenge of nanomaterials can be minimized by (i) transforming 2D nanomaterials into nanocomposites and (ii) surface modification of 2D nanomaterials, owing to their excellent interfacial interaction between the surface of 2D nanomaterials and polymer matrices. Surface modification of nanomaterials (SMNs), compared to unmodified nanomaterials, has attracted a considerable interest in science communities.

Table 1. List of different water pollutants with their sources and adverse effects.

Water Pollutants	Sources of Pollutants	Effects of Pollutants	References.
Pathogens	Viruses and bacteria	Cause water borne diseases which can affect anyone. Those at high risk are infants, younger children, the elderly and patients with underlying illnesses (diabetes, chronic diseases of heart disease and kidney).	[14]
Agricultural Pollutants	Agricultural chemicals	Directly affect the freshwater resources and can cause health-related problems contributing to blue baby syndrome leading to the death in infants.	[15]
Sediments and suspended solids	Land cultivation, demolition, mining operations	Affect water quality and bring about toxicity on fish life and involve reduced oxygen transfer at the gills, reduced ability to clear sediment from the gills and diminished bloodstream.	[16]
Inorganic pollutants	Metals compounds, trace elements, inorganic salts, heavy metals, mineral acids	Cause several human health–related problems on the flora and fauna of the Earth system such as abnormal growth, high risk of cancer, diabetes and obesity.	[17]
Organic pollutants	Detergents, insecticides, herbicides	They are resistant to degradation and tend to bioaccumulate within the food chain. Cause various negative health issues including cancer, immune system suppression, decrements in cognitive and neurobehavioral function, and at least some of them increase the risk of chronic diseases, such as hypertension, cardiovascular disease and diabetes.	[18]
Industrial pollutants	Municipal pollutant water	Cause air, water and land pollution leading to many environmental problems, illnesses and loss of life.	[19]
Radioactive pollutants	Different Isotopes	Exposure to high levels of radiation causes acute health problems like bones, teeth, skin burns and cancer as well as cardiovascular disease.	[20]
Nutrients pollutants	Plant debris, fertilizer.	Cause serious environmental and human health issues which influence the socio-economic issues. Causes algae to grow and expand higher than ecosystems can handle.	[21]
Macroscopic pollutants	Marine debris	Macroscopic pollutants are non-biodegradable materials which cause garbage wastes and plastic pollution.	[22]
Sewage and contaminated water	Domestic wastewater	Causes the quality of the water to worsen, water borne diseases and affects aquatic ecosystems.	[23]

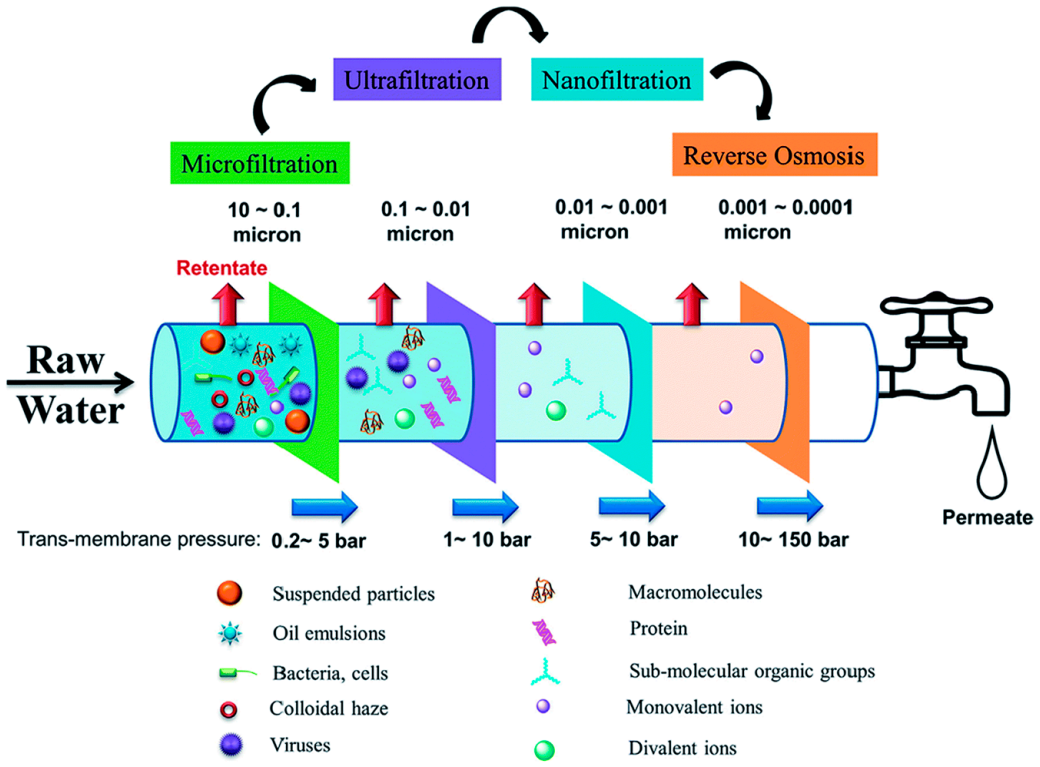

Figure 1. Trans-membrane pressure processes for water treatment technologies with different pore sizes. Reproduced with permission from Reference [13]. Copyrights 2018, Elsevier Science Ltd.

Nanocomposites are multi-phasic materials, in which at least one of the phases shows dimensions in the nano range of 10–100 nm [24,25]. Currently, these materials have emerged as alternatives to overcome deficiencies of different engineering materials and are said to be the 21st century materials, due to their design uniqueness and property combinations which are different from conventional composites. Nanocomposite materials can be classified according to their primary phase (matrix) and secondary phase (reinforcing filler) [26,27]. Among different nanocomposites, polymer-based nanocomposites (PNCs) have become a noticeable field of current research interest and innovation development. PNCs have a lot of advantageous multifunctional properties such as film forming ability, dimensional variability, and activated functionalities [8,28]. Generally, the properties of PNCs are strongly related to the type of polymer matrix and the extent of dispersion of nanomaterials incorporated into the polymer matrix, as well as interfacial interactions between the polymer and nanomaterials [29–31]. The improved interfacial interactions of the nanomaterials with pure polymer change the overall morphology leading to synergistic effects in the nanocomposite properties. The accomplished properties are much better than the individual constituents. Finally, the properties of the PNCs are directly dependent on the volume fraction of nanomaterials, aspect ratio, alignment in matrix and other geometrical factors [32,33]. The main challenges in the development of superior PNCs are (i) the selection of appropriate nanomaterials that possess specific interfacial interaction, (ii) compatibility of nanomaterials with polymer matrix and (iii) suitable processing method to evenly disperse and dispense these nanoparticles within a polymer matrix. The impact of polymer nanocomposites (PNCs) in wastewater treatment can be recognized by an uninterrupted rise in publications over the past ten years. This is contrary to the less extensively instigated environmental impacts of nanomaterials in polymer nanocomposites in water purification (Figure 2).

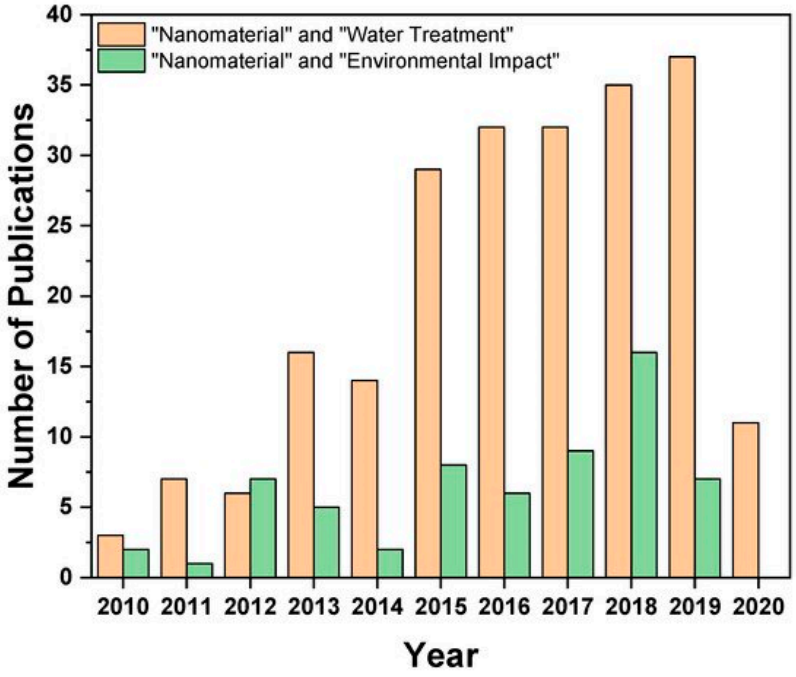

Figure 2. Number of publications in polymer nanocomposites (PNCs) and water treatment. Reproduced with permission from Reference [34]. Open Access 2020, MDPI Water.

In this review, we focus on the comparison of 2D nanomaterials such as layered double hydroxides (LDHs) and other nanoclays in polymer-based nanocomposites (PNCs), their preparation methods and multifunctional properties and their use for water purification. The primary goal is to highlight an optimal efficiency of LDHs and other nanoclays adsorption capacities and recent progress of nanomaterials in decontamination ability of various pollutants with selectivity including practical and potential applications.

2. Comparison of Other Nanoclays and LDHs Crystal Structures

2.1. Other Nanoclays Crystal Structure

Nanoclays (NCs) are a broad class of naturally occurring inorganic minerals optimized for use in polymer-clay nanocomposites for water purification and environmental protection. NCs are versatile and two-dimensional (2D) building blocks for multifunctional material systems with several property enhancements targeted for many applications. Based on their chemical composition and particle morphology, clay minerals are categorized into many classes such as smectite, chlorite, kaolinite, illite and halloysite. Nanoclays have been studied and developed for various applications [29,31,35] and are abundantly available, very cheap and low environmental impact. Clay minerals are members of the phyllosilicate or sheet clay silicates consisting of hydrated alumina–silicates and can be used as natural nanomaterials or nano-absorbent since the dawn of nanotechnology [36]. Nanoclays are nanoparticles of layered mineral silicates with layered structural units that can lead to the formation complex/multifaceted clay crystallites by stacking these layers [37]. The basic building blocks of clay minerals are tetrahedral silicates and octahedral hydroxide sheets [38]. Octahedral sheets consist of aluminum or magnesium in a six-fold coordination with oxygen from a tetrahedral sheet and with hydroxyl (Figure 3). Tetrahedral sheets consist of silicon–oxygen tetrahedra concomitant to neighboring tetrahedral sharing three corners, while the fourth corner of each tetrahedron sheet is connected to an adjacent octahedral sheet via a covalent bond.

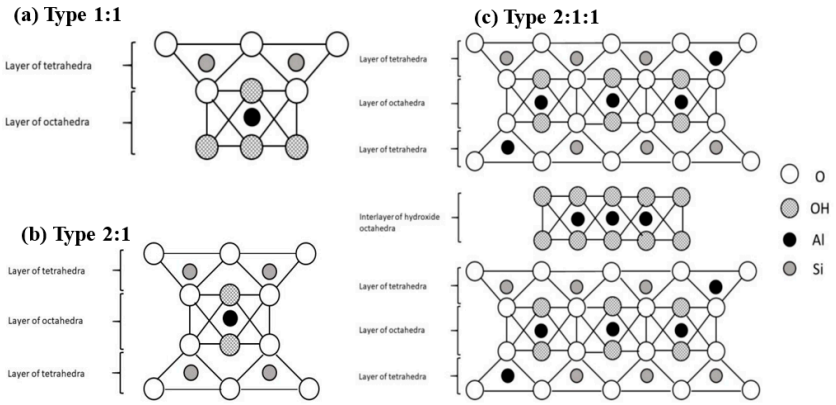

Figure 3. The layer phyllosilicate structures: (**a**) Type 1:1, (**b**) Type 2:1, and (**c**) Type 2:1:1. Reproduced with permission from Reference [39]. Open Access 2019, MDPI Animals.

The arrangements of these sheets influence a number of contributing factors in clay silicates. Based on their mineralogical composition, there are nearly thirty different types of nanoclays used in various applications [40,41]. Table 2 depicts three major types of phyllosilicates which are distinguished as 1:1 layer type (T-O), 2:1 layer type (T-O-T) and 2:1:1 layer type (T-O-T:O) common in nanoclay materials. In 1:1 lattice structures (T-O), each tetrahedral is connected to one octahedral sheet, while in 2:1 lattice structures (T-O-T), each octahedral sheet is connected to two tetrahedral sheets, one sheet on each side. Lastly, in 2:1:1 lattice structures (T-O-T:O), each octahedral sheet is adjacent to another octahedral sheet and connected to two tetrahedral sheets [31,42–44].

Table 2. Classification of clay minerals and their characteristics.

Clay Minerals Group	Layer Type Ratio	Characteristics	References.
Rectorite, Kaolinite, Halloysite, Chyrsotile.	1:1 (T-O) Dioctahedral	Non-expansive, no layer charge and very little isomorphic substitution.	[41,42]
Smectite Vermiculite	2:1 (T-O-T) dioctahedral Trioctahedral	Highly expansive, low layer charge moderately expansive, Intermediate layer charge. extensive isomorphic substitution.	[43]
Pyrophylite talc, mica, brittle mica.	2:1 (T-O-T) dioctahedral Trioctahedral	Non-expansive, high layer charge, extensive isomorphic substitution.	[43]
Chlorite	2:1:1 (T-O-T-O) dioctahedral Trioctahedral Di, Trioctahedral	Non-expansive, high layer charge, extensive isomorphic substitution.	[31,44]

Halloysite nanoclay is an aluminosilicate nanotube naturally occurring clay material with the average dimensions of 15 nm × 1000 nm [45]. This halloysite nanoclay has (1:1-layer type) and the hollow tube structure is primarily utilized in medical applications, food packaging industry and rheology modification [46]. The most commonly used nanoclay in materials applications is plate-like montmorillonite (MMT) material. This MMT has approximately 1 nm of aluminosilicate layers which are surface coated with metal cations in a multilayer stacks of ~10 µm. Depending on surface modification of the clay layers, MMT can be dispersed in a polymer matrix to form polymer-clay nanocomposites with applications such as, flame-resistance, solidifying agents, water purification and gas permeability modification. MMT clay layers with 2:1 layered silicates of T-O have high cation exchange capacity (CEC) on the siloxane surface that can interact well with different substances like

organic or biological molecules [47,48]. The MMT nanoclay stacks have attracted a lot of interest because of outsized surface area, swelling behavior and high cation exchange capacity [49,50]. Unlike MMTs, halloysite materials are easily dispersed in many polymers showing no exfoliation due to scarcity of OH groups on their surfaces. In addition, these tube-like nanoclays are excellent nanomaterials for numerous chemical molecules [51]. Therefore, the modified clays are used as effective reinforcing phase for polymers to improve their mechanical and thermal properties. Nanoclays acting as carriers continuously and constantly released some active molecules such as flame-retardants, antioxidants, anticorrosion and antimicrobial agents [52,53]. In recent years, the research and development of novel polymer/nanoclay composites for water purification has attracted a lot of attention in the field of material chemistry [54]. Rigid nanoclay like layered double hydroxides (LDHs) must be used as an effective reinforcing filler to polymer structures and impede the polymer chains free movement adjacent to the filler [29–31,54].

2.2. Layered Double Hydroxides (LDHs) Crystal Structure

Layered double hydroxides (LDHs) also known as hydrotalcite (HT)-like materials are a class of synthetic two-dimensional (2D) nanostructured anionic clays with a highly tunable brucite [$Mg(OH)_2$]-like layered crystal structure (Figure 4). These inorganic materials contain layers of positively charged metal hydroxides with multivalent anions for neutrality. The LDHs are generally represented by formula

$$[M^{2+}_{1-X}\, M^{3+}_{X}(OH)_2]^{X+}[A^{n-}]_{X/n}\, mH_2O \quad (1)$$

In this formula, M^{2+} and M^{3+} represent the divalent and trivalent layer cations, respectively. A^{n-} is the exchangeable anion such as OH^-, F^-, NO_3^-, Cl^-, CO_3^{2-} and/or SO_4^{2-}. Reasonably stable LDH phases are often observed only when the value of x varies in the range 0.22–0.33 resulting in M^{2+}/M^{3+} molar ratios of 2:1 to 4:1 [55–59]. If x is more than 0.33, then an increased number of neighboring M^{3+} containing octahedra leads to the formation of $M(OH)_3$. If x is less than 0.2, then an increased number of neighboring M^{2+} containing octahedra in the brucite-like sheets resulted in the precipitation of $M(OH)_2$. However, these limits of the value of x must be regarded as the maximum interval, which can be narrower depending on the composition of the LDH.

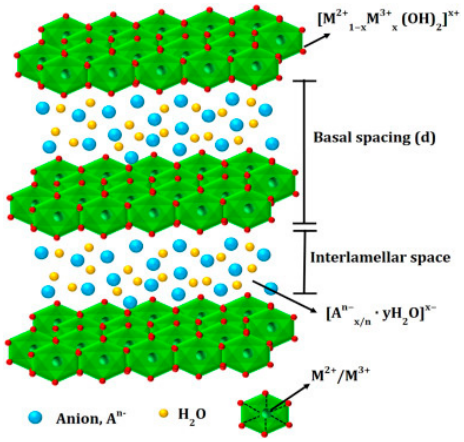

Figure 4. Structure of layered double hydroxide (LDH). Reproduced with permission from Reference [60]. Copyrights 2018, Elsevier Science Ltd.

As result, a large class of isostructural materials, which can be well-thought-out complementary to aluminosilicate clays, with useful physical and chemical properties can be achieved. This can be carried out by changing the nature of the metal cations, the molar ratios of divalent/trivalent cations, and the types of interlayer anions. These compounds are composed of positively charged brucite-type octahedral sheets, interchanging with interlayers containing carbonate anions in the natural mineral or

other exchangeable anions in the synthetic hydrotalcite (HT)-like materials, along with water molecules. The hydrogen bonding associated with the interlamellar water molecules serves as a driving force for the stacking of the clay layers (see Figure 4).

2.3. An overview of Preparation Methods of LDHs

In the last few decades, a number of studies associated with the synthesis of LDH have been reported and some are easy and simple to process for many industrial applications. Various kinds of low cost, environmentally and eco-friendly LDHs can be synthesized by using fundamental methods of choice. These commonly used methods include co-precipitation; ion exchange; reconstruction; sonochemical method; hydrothermal/solvochemical method; sol–gel method; induced hydrolysis method; and urea method [57,59–65].

2.3.1. Co-Precipitation Method

Co-precipitation method is also referred to as a large-scale and direct technique typically utilized for the synthesis of LDH platelets with different divalent and trivalent cations (M^{2+} and M^{3+}) coupled with many inorganic anions (Cl^-, NO_3^-, CO_3^{2-}) and organic molecules/outsized biomolecules [57]. In this co-precipitation method, a dropwise addition of alkali solution into the divalent and trivalent layer cations/mixed metal salts containing solution in a proper ratio resulted in formation of LDH as shown in Figure 5. During this method, a pH emerged as a very crucial factor which negatively influences both the structural and chemical properties of LDH component to a larger extent. In a dropwise addition, the pH of the reaction mixture is maintained constantly at the range of 8–10 and purged at N_2 atmosphere in an attempt to achieve high chemical homogeneity in LDH [61]. The resulting solution mixture is allowed to stay for a long period of time in order to obtain a reproducible and well-crystallized LDH structural material. The obtained precipitate is collected by filtration, washed thoroughly with deionized water and dried in an oven overnight. The underpinning principle of co-precipitation is based on a simple, economical and industrially feasible technique utilized for the synthesis of metal oxide materials in solution. This led to the brucite-like layers' formation, which uniformly dispersed metallic cations and inorganic anions.

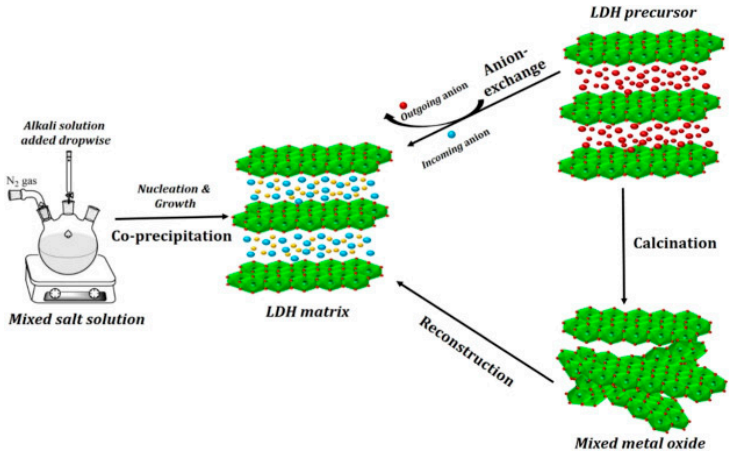

Figure 5. Schematic representation of co-precipitation, ion exchange and reconstruction methods LDH. Reproduced with permission from Reference [59]. Copyrights 2018, Elsevier Science Ltd.

2.3.2. Ion Exchange Method

Anion-exchange method is better for the incorporation of layered silicates into a solution containing anions species ready for exchange as compared to other methods. The ion exchange method (Figure 5) is based on the exchange of anions in interlayer space with other anionic species. In this method, the precursor LDH is suspended in an aqueous solution containing the anionic species to be exchanged.

The suspension is then stirred constantly for several hours at room temperature. The solid precipitate is then collected by filtration, washed several times with deionized water and dried in an oven overnight. Furthermore, the interlamellar region can also contain water molecules and is referred to as internal water dominant region where water molecules are organized by the inorganic layers via hydrogen bonding. The high anion exchange capacity of LDH matrix-like compounds produces their interlayer ion exchange by outgoing anions and incoming useful anions, easily accomplished and reflected in LDH precursor product formation [62] (Figure 5).

2.3.3. Reconstruction Method

As shown in Figure 5, this reconstruction method is a well-known regeneration or memory effect method of LDH. According to this method, the layered structure of brucite-like LDH with carbonate anion is used as a precursor during hydration and calcination due to its behavioral pattern. The reconstruction method is based on the memory effect or regeneration which is one of the unique properties of LDHs. In first step, the calcination of LDHs is performed at a particular temperature to obtain mixed metal oxides (Figure 5) and then subjected to rehydration in aqueous solution with the anion to be intercalated [63]. The solid precipitate is collected by filtration, washed several times with deionized water and dried in an oven overnight. The structural recovery, however, depends upon some experimental conditions such as, calcination temperature, duration and rate of heating. The reconstruction method is useful mainly in the preparation of large organic anions intercalated LDH [63,64].

2.3.4. Sonochemical Method

In sonochemical method, LDHs are prepared by co-precipitation method followed by sonochemical treatment. In first step, the co-precipitation method is performed to the latter as explained fully under Section 2.3.1 above. In the second step after successful completion of mixing, the resultant solution is subjected to ultrasound irradiation at a given time and temperature. The solid precipitate is filtered, washed thoroughly with deionized water and put in an oven overnight for further drying. This sonochemical method is best described as a synthetic and high intensity ultrasonic/three-fold acoustic cavitation phenomenon which assist in improving the crystallinity of LDH phases [61,65]. When the solution mixture is subjected to ultrasonic irradiation, rapid movement of the fluid leads to three-fold acoustic cavitation phenomenon (Figure 6) in which microbubbles undergo nucleation formation, growth and implosive collapse [65]. The formation of microbubbles produced a distinctive hot spot due to the compressional heating induced by collapsing of bubble and therefore yields the bubble with extremely high temperature, pressure and cooling rates [66].

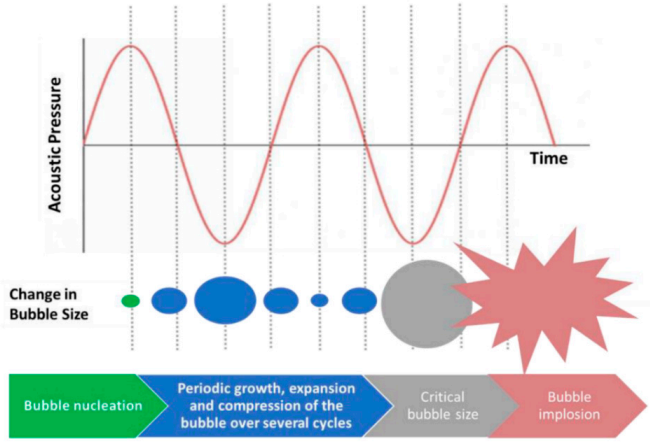

Figure 6. Schematic representation of three-fold acoustic cavitation phenomenon. Reproduced with permission from Reference [67]. Open Access 2020, MDPI Energies.

2.3.5. Hydrothermal/Solvothermal Method

The hydrothermal synthesis method illustrated in Figure 7a,b is similar to the co-precipitation method. In this method, two solutions containing M^{2+} and M^{3+} metal salts are added dropwise to another solution containing base under vigorous stirring at room temperature. Thus, the suspension is transferred into a Teflon-lined autoclave and heated at higher temperature (100–180 °C) for many hours (10–48 h) based on the metal ions [68]. The pH of the supernatant solution is in the threshold range of 8–10. The solid precipitate is collected by centrifugation washed thoroughly with deionized water and ethanol and dried in an oven overnight. The hydrothermal method is useful for synthesis of highly crystalline LDHs with uniform morphology compared to co-precipitation technique [69]. Solvothermal method is a synthesis method where a chemical reaction takes place in a closed solvent system at elevated temperatures above the boiling point and standard pressures. In a typical solvothermal synthesis, the amount of organic solvent such as glycerol or alcohol is used in a non-aqueous solution at somewhat high temperatures, while hydrothermal method refers to synthesis via chemical reactions in aqueous solution just above boiling point of water in a closed vessel. Many scientists realized the importance of preparing inorganic nanomaterials using hydrothermal and solvothermal reactions, upon which effective syntheses of novel high-technology and green materials would be established. The main reason for this remarkable and milestone achievement in preparing nanomaterials is the easy of processing which include low temperature process, low energy consumption, no harm to the environment and more importantly high degree of crystallinity of the material can easily be produced [68,69].

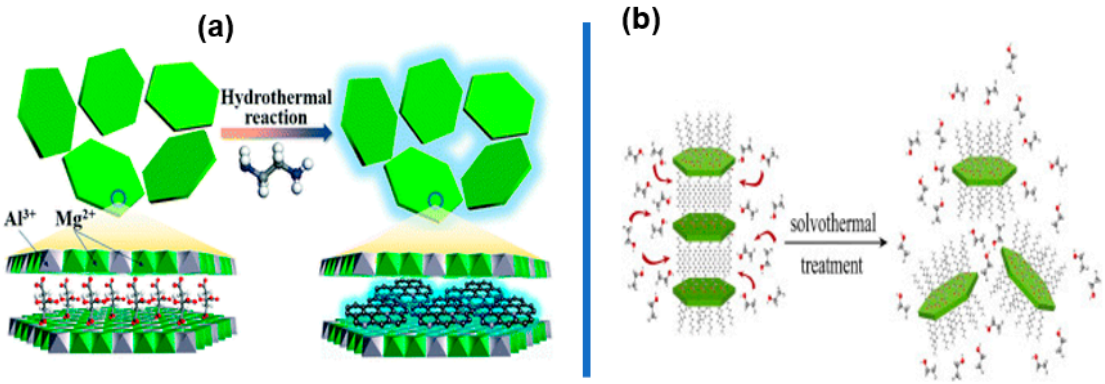

Figure 7. Schematic representation of (**a**) hydrothermal method and (**b**) solvothermal treatment of layered double hydroxide (LDH). Reproduced with permission from Reference [70,71]. Copyrights 2017 and 2019, RSC and Elsevier.

2.3.6. Adsorption and Layer-by-Layer Method

In this case, adsorption (Figure 8a) can be referred to as the adhesion of divalent and trivalent ions (M^{2+} and M^{3+}) from a liquid or dissolved solid to surface of the LDH adsorbent. This creates a film of the adsorbate over the surface in many processes such as chemical, physical, biological and natural systems and widely used in various industrial applications [72]. The adsorption process may occur through weak van der Waals forces (physisorption) or covalent bonding (chemisorption) and also may occur due to electrostatic attraction between the adsorbate and surface of the adsorbent. It is a surface phenomenon most widely adopted in wastewater treatment for removal of various organic contaminants from aqueous solution.

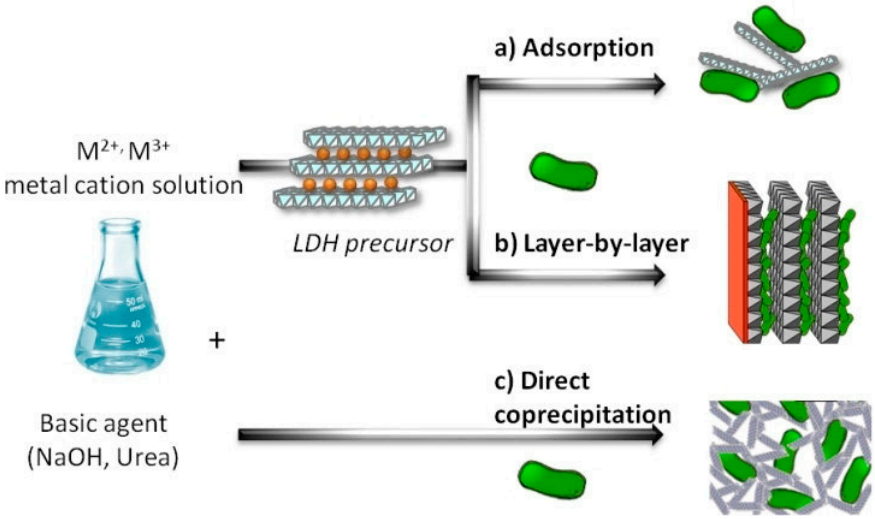

Figure 8. Schematic representation of (**a**) adsorption method, (**b**) layer-by-layer deposition and (**c**) direct co-precipitation method of layered double hydroxide (LDH). Reproduced with permission from Reference [73]. Copyrights 2018, John Wiley and Sons.

Layer-by-layer (LBL) assembly (Figure 8b) is a universal method for coating substrates with polymers, colloids, biomolecules, and even cells. This presents superior control and versatility when compared to other thin film deposition techniques in certain research and industrial applications. The LBL technique is known to support electrostatic interactions between positively charged layers and negatively-charged molecules and leads to nanostructured thin films [74]. This LBL deposition technique has three types of methods known as (i) the dipping layer-by-layer deposition technique (dipping-LBL); (ii) spray layer-by-layer deposition method (spray-LBL) and (iii) spin layer-by-layer deposition method (spin-LBL) method. Dipping-LBL is executed by chronologically adsorbing opposite charged materials onto a substrate via enthalpic and entropic driving forces [75]. In this method, the time depends on both the diffusion and adsorption of molecules, solutions or suspensions. Spray-LBL is a deposition technique where divalent and trivalent solutions are sprayed onto a vertical substrate, and the layer is formed after completion of drying in an oven overnight [58]. In spin-LBL method, the solutions or suspensions are deposited on a substrate attached to a spin coater, and the rotation speed generates a high centrifugal force. Thus, high rotational speed with high airflow rate at the surface leads to fast drying times of the liquid which in turn quickly and easily produce very uniform layers or thin films. In both spray-LBL and spin-LBL methods, the total time does not depend on the diffusion of molecular species. The co-precipitation method shown in Figure 8c has already been previously explained in Section 2.3.1.

2.3.7. Sol-Gel Method

The sol-gel method is a low-cost, simple preparation method and efficient wet-chemical method of high-purity metal oxide materials from LDH precursors through hydrolysis and condensation processes [76]. In this method (Figure 9), the mixed salt solution of $Al(NO_3)_3{\cdot}9H_2O$ and $Mg(NO_3)_2{\cdot}6H_2O$ and alkali solution of NH4OH were concurrently added to a beaker and heated under refluxed condition. The pH of the suspension is maintained at 8–10 by adding NH4OH base under magnetic stirring at ambient temperature until the gel formation is achieved. The resultant gel like product is filtered, washed properly with deionized water via re-dispersion/centrifugation and dried overnight. The formed gel was re-dispersed in water by ultra-sonication to produce LDH single layer nanosheets (SLNSs) dispersion. A portion of the LDH SLNS gel was further tried in an oven at 80 °C for 24 h to yield a well-crystallized LDH SLNS sol sample. The LDHs synthesized using sol-gel method is thermally very stable, but less crystalline than those synthesized via the co-precipitation method.

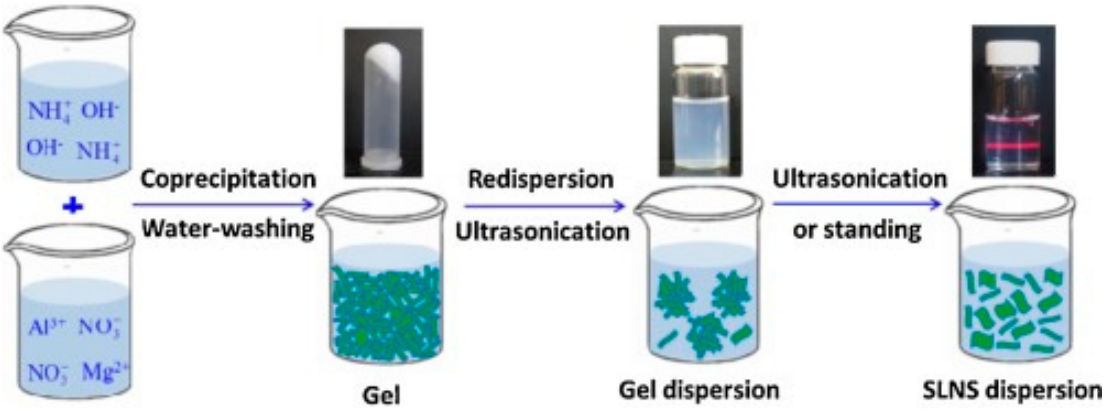

Figure 9. Schematic representation of sol-gel method of layered double hydroxide (LDH). Reproduced with permission from Reference [77]. Copyrights 2016, Elsevier.

2.3.8. Induced Hydrolysis Method

In this method, metal oxides are added dropwise to an acidic solution containing M^{3+} metal salts. The metal oxides are dissolved progressively in the acidic solution and precipitated into LDH. The pH is cushioned at 8–10 by the oxide suspension [59]. The obtained solid precipitate is collected, filtered, washed methodically with deionized water and dried at 80 °C for 24 h. This method of induced hydrolysis can also be used for synthesis of LDH with di-divalent, di-tetravalent and tri-trivalent systems.

2.3.9. Urea Method

In general, urea is added to an aqueous solution of preferred M^{2+} and M^{3+} metal salts and heated under reflux condition for several hours. The precipitate product is collected by filtration, washed thoroughly with deionized water and dried overnight. The rate of urea hydrolysis can possibly increase significantly with an increase in the reaction temperature to 100 °C [59]. The urea molecules undergo degradation to form ammonium carbonate, which initiates the precipitation into LDH with CO_3^{2-} as interlayer anion. This urea method provides high degree of crystallinity and a fine particle size distribution. Urea-based co-precipitation provided the better crystallinity and particle size due to thermal treatment and hydrolysis of urea which is proceeded in a very slow manner [57,59,60].

In comparison to many other nanoclays or layered materials, LDHs have compositional multiplicities in the cationic layers and in the hydrated interlayer of anions for charge balance which lead to some functional diversities. This implies that LDHs among layered materials have the great advantages and number of possible compositions, metal-anion combinations and morphologies useful for synthesis and processing methods. Apart from that, LDHs can be used in a variety of potential applications due to their anion exchangeability, compositional flexibility, good biocompatibility, low cost, facile synthesis, pH dependent solubility, thermal stability and high chemical versatility [78]. Due to their tunable chemistry and high charge density tailored properties, LDHs have attracted great attentions in various technologically significant fields and applications such as production of renewable energy [4,21,29], adsorbents [7,41,79], water purification [8–10,80,81], antimicrobial activities [10,24], sensors [29,82–84], flame resistance [48], drug delivery [85,86], cosmetics [87,88] and environmental catalysis [57,89,90]. In our previous work [91], detailed discussion about various applications were made and the current work focuses more on water purification.

2.4. Preparation Methods of Polymer-Clay Nanocomposites (PCNCs) and Surface Modification

The manufacturing of PCNCs depends mainly on a proper method selection which ensures acceptable level of dispersion of the nanofillers throughout the polymer matrix. Several processing methods were employed in preparing polymer-based clay nanocomposites such as in situ polymerization, the melt blending, and solution blending techniques [92,93] (see Figure 10). In each preparation method, an absolute goal is to achieve a desired uniform dispersion of nanoclays in the pristine polymer matrix. However, there are currently numerous interesting views about the applications and usage of these methods. According to the following studies [18,94,95], melt blending is regarded as a significantly, industrially viable and ecofriendly technique with high economic potential for preparation of polymer–clay nanocomposites. The in situ polymerization method is a commonly used synthesis technique and easy to modify by changing the polymerization conditions [96] and provides uniform dispersion. Both these methods require either a large amount of organic solvent or high viscosity or thermally unstable polymers at high temperatures. In comparison to melt blending, the solution-blending technique often produces pleasing dispersion of clay layers in the polymer matrix [31] due to its low viscosity and high agitation power. Each technique has its own relevant significance and limitations in relation to certain required industrial applications.

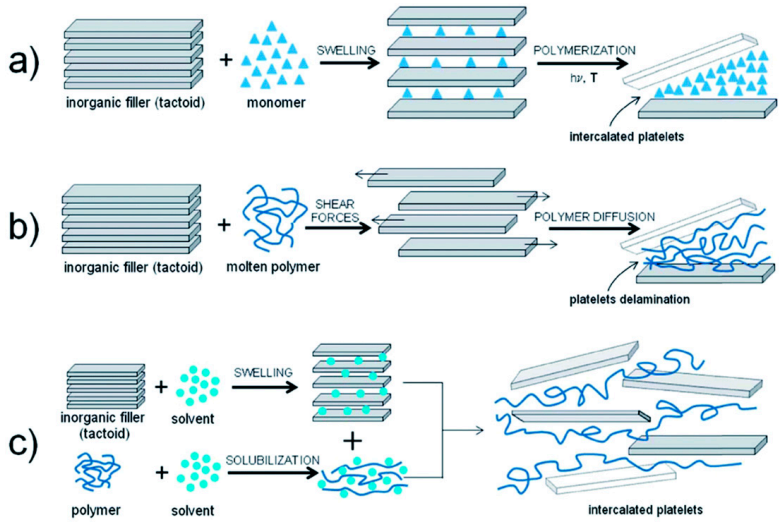

Figure 10. Illustration of (**a**) in situ polymerization, (**b**) melt intercalation and (**c**) solution intercalation. Reproduced with permission from Reference [97]. Open Access 2014, Royal Society of Chemistry.

2.4.1. In Situ Polymerization Technique

Due to the silicate dispersion deduced information, in situ polymerization is more effective in the preparation of composites and can sidestep the harsh thermodynamic requirements related to the polymer intercalation process [18,31,98] (Figure 10a). Furthermore, this polymerization technique (i) tolerates resourceful molecular strategies of the polymer matrix; (ii) it provides an effective approach to the synthesis of different polymer/nanoclay composites with prolonged property range and (iii) facilitates the development of the interface between the filler and the polymeric matrices by modification of the matrix composition and structure. Many studies focus on preparing novel polymer/nanoclay composites via the in situ polymerization method and demonstrate the benefits of this method in comparison with other types of synthesis methods [18,31,98,99]. For instance, Ozkose et al. [100] investigated the synthesis of poly(2-ethyl-2-oxazoline)/nanoclay composites for the first time using in-situ polymerization. In their finding, a ring-opening polymerization method was applied, which then initiated the delamination of clay layers in the polymer matrix and led to a composite formation.

2.4.2. Melt Blending Technique

Melt blending technique involves direct mixing of layered clay into the molten polymer matrix and can either be immobile or active. In an immobile melt blending (melt annealing), the process is performed under a vacuum at temperatures of approximately 50 °C above transition temperatures in the absence of mixing. In an active melt blending, the polymer melting is performed during a melt mixing in the presence of an inert gas [27,101]. As a result, the polymer clay nanocomposites are produced from the enthalpic driving force and influence of the polymer–organoclay interactions. The melt-mixing method (Figure 10b) provides better mixing of the polymer and nanoclay fillers and is well-suited with current industrially and ecofriendly viable processes such as extrusion and injection molding for thermoplastic and elastomeric material manufacturing. The absence of solvents reduces the environmental impact and minimizes potential interactions between the host and polymer solvents, which, in many cases, limits clay dispersion [18,102–104].

2.4.3. Solution Blending Technique

Solution-blending is a solvent based process in which the polymer and the prepolymer are soluble, which causes swelling of the clay layers, see Figure 10c. This technique involves thoroughly dispersing the layered silicate within appropriate solvents, which includes polymer/soluble prepolymer. These clay layers are dispersed into the solvent and further mixing with a dissolved polymer would be done to prepare the solution which allows polymer chains to be embedded into the exfoliated clay layers. Upon reaction completion stage, the solvent molecules would have evaporated, trapping the polymer chains intercalated into the gallery of clay interlayers [105,106] and the matrix segments combine with the dispersed clay layers.

The major driving force of intercalation process in solution mixing is the increased total disorder of the system referred to as desorption process of solvent molecules. This entire process normally consists of three stages known as (i) the dispersion of clay in a polymer solution, (ii) well-ordered solvent removal and (iii) lastly composite film casting [102,106,107]. The dispersion of clay in neat polymer necessitates active agitation such as stirring, reflux and shear mixing.

It is well documented that the morphology and dispersion of clay nanoplatelets in polymers is one of the key factors affecting their gas barrier properties [95,108]. One of the most vital challenges in the preparation of polymer/clay nanocomposites with improved barrier performances [95] is to achieve high level of exfoliation and orientation. In general, polymer/clay nanocomposites may result into three possible morphologies referred to as (i) phase-separated, intercalated and exfoliated structures (see Figure 11) [95]. For attainment of phase-separated nanocomposites, clay tactoids are formed throughout the pure polymer matrix, and no separation of clay nanoplatelets occurs. Polymer chains surround clay nanoplatelets but do not penetrate between the clay layers [109] and absence of platelets separation may result in large, micron-sized agglomerates. In intercalated nanocomposties, some of the polymer molecular chains have penetrated the interlayer galleries of the clay tactoids. Due to the penetration of polymer molecular chains, the spacing between individual clay platelets and the overall order of the clay layers is increased and maintained [110]. In exfoliated nanocomposite structures, the clay nanoplatelets are fully separated and dispersed uniformly within the continuous polymer matrix. Exfoliated nanocomposites produce the highest surface area interaction between clay nanoplatelets and neat polymer [111]. After a successful exfoliation, an enhancement in properties can be manifested in barrier properties, as well as improved mechanical properties, decreased solvent uptake, increased thermal stability and flame retardancy [112,113].

However, the main drawback to achieve homogeneous dispersion of most inorganic clays within organic polymers is closely related to the incompatibility between hydrophilic clay and hydrophobic polymer, which often causes agglomeration of clay mineral in the polymer matrix. Thus, surface modification of clay minerals for a good compatibility with the polymer is the most important step to achieve homogeneous dispersion of clay nanoplatelets in polymer matrix [29,31,76,109].

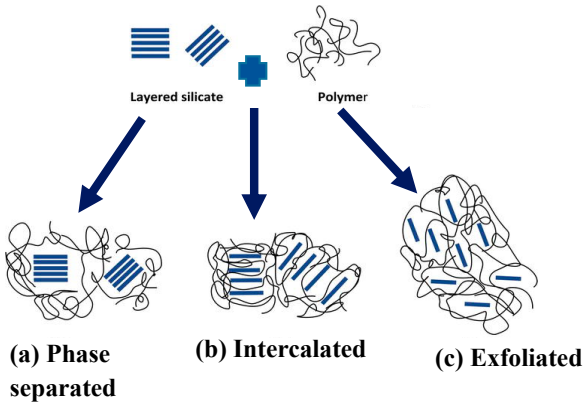

Figure 11. The main types of nanocomposites: (**a**) intercalated, (**b**) flocculated and (**c**) exfoliated. Reproduced with permission from Reference [113]. Open Access 2018, IntechOpen.

2.4.4. Surface Modification of Nanoclays and LDHs

Layered silicates including nanoclays and layered double hydroxides (LDHs) can be intercalated with hydrophilic polymers such as thermoplastic, thermosetting and elastomeric polymers. Most commonly used polymers are hydrophobic, while others such as poly(vinyl alcohol) (PVA), poly(ethylene glycol) (PEG), poly(acrylic acid) (PAA), poly(2-oxazoline) (POX), poly(methyl methacrylate) (PMMA), poly (ethylene-co-vinyl acetate) (EVA) are hydrophilic in nature. Despite their various applications, silicate layers also have one primary drawback due to the intrinsic incompatibility of hydrophilic silicate minerals and the hydrophobic polymer matrix. The incorporation of hydrophilic silicate minerals into a hydrophobic polymer causes agglomeration/aggregation, which lead to incompatibility between the components and weak extent of dispersion. Thus, it is indispensable to augment the degree of dispersion and the compatibility between the polymer matrix and the clay by surface modification [114]. The miscibility between layered silicates and the polymer matrices is enhanced as the clay becomes hydrophobic after surface modification using organic materials. For fabrication of layered silicates with engineering polymers such as thermoplastic or thermosetting, the surfaces of the layered silicate have to be modified by ion-exchange processes using cationic surfactants like quaternary alkylammonium salt, alkylphosphonium-based positively charged species or coupling agents [49]. The surface energy of layered silicates is reduced due to the modification, providing the efficiency and reinforcing characteristics in controlling the stability of the polar polymer matrix [105]. As a result, the interlayer spacing increases to high margins, producing better anchoring of the polymer chains for improvement of the overall properties of the system. The most preferential modification is the addition of coupling agent such as silane, which ensures good compatibility or chemical bonding with polymers, an exchange of the interlayer inorganic cations such as Na^+ with organic ammonium cations. In addition to ionic modifications, covalent and dual modifications (ionic and covalent are possible [115]. Other approaches, such as grafting polymer chains directly onto the surface of a nanoclay or using non-ionic surfactant have also been used [116]. There are two ways of ionic modification, called directly reacting anionic or cationic surfactants with the nanoclay or using ionic liquids. Imidazolium, pyridinium, trihexyltetradecylphosphonium tetrafluoroborate, and trihexyltetradecylphosphonium decanoate salts are commonly used for ionic liquid modification of nanoclays which show better properties [117–122]. The modified clay is commonly referred to as organoclay and the schematic illustration for the modification of clay particles is shown in Figure 12.

Chang et al. [119] prepared and characterized bio-oil phenolic foam (BPF) and surfactant modified bio-oil phenolic foam (MBPF) reinforced with Montmorillonite (MMT) as secondary phase. Their findings showed remarkably enhanced toughness as well as good flame resistance and improved the thermal stability of modified bio-oil phenolic foam (MBPF)-MMT nanocomposite foams compared to unmodified BPF-MMT nanocomposites. Covalently modified clay silicate is often synthesized via a

step-reaction polymerization called condensation polymerization. During this process, the reaction is taking place between the hydroxyl groups from the surface of clays with mono- or tri-alkoxy silanes such as methoxy(dimethyl)octylsilane, tri-alkoxy silanes, trimethoxy(octyl)silane, (3-aminopropyl) triethoxysilane and others. The covalent modification renders the clay surface more hydrophobic [120]. Uwa et al. [121] studied the effect of nanoclay as reinforcing agent on the mechanical properties and thermal conductivity of polypropylene (PP) and maleic-anhydride-grafted-polypropylene (MAPP). The results of PP/MAPP/nanoclay composites exhibited a significant improvement in tensile strength and stiffness with low clay contents. Thermal conductivity analysis revealed that composites with high clay loadings have high resistance to heat. Twofold modifications can be done possibly by first covalently modified clay silicate followed by an ionic modification or vice versa. In comparison to single modifications (either ionic or covalent), dually modified clays show even more improved properties in terms of mechanics, thermal stability, dimensional stability, and viscoelastic characteristics.

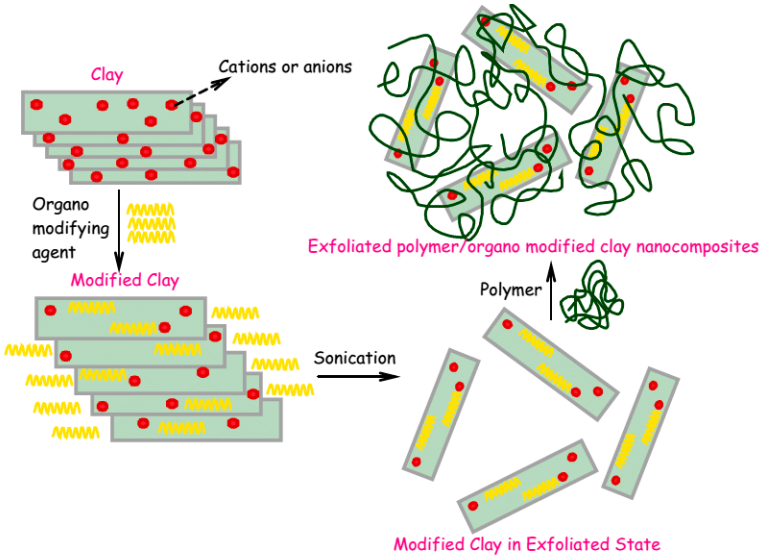

Figure 12. Schematic representation for the preparation of exfoliated polymer/organomodified clay nanocomposites. Reproduced with permission from Reference [122]. Copyrights 2017, Elsevier Ltd.

Various polymer-based layered silicates nanocomposite systems have been investigated, and their methods, structure and properties are compared and summarized in Table 3. The comparison of polymeric categories such as thermoplastic, elastomeric and thermoset matrices including thermoplastic polyurethane (TPU), polyisoprene (PIP), nacre-thermoset, poly(L-lactic acid) (PLLA), polypropylene (PP), polyamide 11 (PA11), nitrile butadiene rubber (NBR), styrene-butadiene rubber (SBR), Vinyl ester (VE), epoxy (EP), polylactic acid (PLA), Polybutylene terephthalate (PBT), polymethyl methacrylate (PMMA) reinforced with corresponding LDHs and other nanoclays are also included in Table 3 summary. Nevertheless, it is evident in the literature that the polymeric-thermoplastic matrices are utilized more preferentially over the thermosets because of their features such as light weight, can be re-melted/molded, and shaped. Recently, there is a growing demand to safeguard and deal with environmental contaminants and pollutants in preparation of biodegradable matrix/LDHs nanocomposites which are referred to as eco-friendly materials. Layered double hydroxides (LDHs) systems appeared to have better overall properties than most of other nanoclays due to their varied chemical compositions and methods of synthesis. LDHs possess higher layer charge densities and prefer multivalent anions within their interlayer space due to strong electrostatic interactions between the brucite-type sheets and the anions. Therefore, swelling is more difficult in LDHs than for other clay minerals. In short, LDHs containing monovalent anions like nitrate or chloride ions are viewed as good precursors for exchange reactions with charge balance, which lead to some functional diversities.

Table 3. Comparison of polymer-unmodified/modified layered double hydroxide and other nanoclays for water purification.

Polymer-Category	Layered Silicate	Processing Methods	Observed Morphology and Removal of Dyes or Other Heavy Metal Pollutants	References.
Polyacrylamide (PAM)-thermoset	Sodium-montmorillonite (Na-MMT)	Free-radical cross-linking Polymerization (In situ polymerization)	A slightly intercalated MMT structure and incomplete exfoliation. PAM/Na-MMT nanocomposites efficiently removed the heavy metal ions such as Ni^{2+} and Co^{2+} wastewater with removal yield between 87.40% and 94.50%.	[123]
N-isopropylacrylamide (NIPAm) nanogel polymer-thermoset	Sodium-montmorillonite (Na-MMT)	Surfactant free dispersion radical crosslinking polymerization	Exfoliated structure. The Na-MMT nanogel composites showed drastic reduction in water surface tension and efficiently remove methylene blue (MB) dye, Co and Ni cations from water within an hour. The prepared Na-MMT nanogels desorbed and reused four times to remove the heavy metal from water with the same efficiency.	[124]
Polyethylene (PE)-thermoplastic	Green clay	Solution mixing	An exfoliation nanocomposite morphology was achieved. The adsorption increased with increasing methylene blue concentration, the pH values and with increasing temperature due to the increased kinetic energies of the molecules. The removal of methylene blue (MB) from water solution was effectively achieved.	[125]
Cellulose-thermoplastic	Montmorillonite (MMT)	Aqueous solution method	Intercalated nanocomposite morphology was observed. The adsorption was not considerably affected by pH due to the presence of hydrophobic interaction between MB and hydrogels. The hydrogel samples containing intercalated clays showed high removal efficiency for MB aqueous solution with concentrations of 10 and 100 mg L^{-1}. The removal efficiency for MB increased with the clay contents of hydrogel networks and was reported as high as 97%.	[126]
PP-Thermoplastic Chitosan (CS)-thermoplastic	Montmorillonite Bentonite	Melt blending technique using twin-screw extruder Both melt compounding and crosslinking reaction between chitosan and glutaraldehyde	Structural morphology of intercalated PP/MMT is observed, while PP-g-MA/MMT appeared to have obtained an exfoliation morphology. Neat PP and synthesized PP-g-MA/MMT nanocomposites were used for removal of heavy metal adsorbent for adsorption of Pb(II) from aqueous solutions. The results revealed that adsorption efficiency of 96% for the removal of Pb(II) ion contaminant with neat PP and 0.5 wt% MMT were attained and conform the Langmuir isotherm. The PP-g-MA/MMT at 0.5 wt% nanocomposites showed can efficiently and effectively be used as super adsorbent for optimized removal percentage of contaminants like Pb(II) ions from wastewater. Intercalated structures and morphology were observed. The adsorption of an azo dye called Amido Black 10B (AB 10B) adsorbate onto the crosslinked chitosan (CCS)/Bentonite (BT) clay composites was reported to be optimal at high temperatures and low pH value of 2. CCS/BT composite is an effective biosorbent for the removal of AB10B from aqueous solutions.	[127,128]
Polyethylene glycol (PEG)-thermoplastic	Mg–Al-layered double hydroxides (LDHs)	Simple chemical precipitation method.	The morphology of the synthesized PEG-modified Fe_3O_4/Mg–Al-layered double hydroxides (LDHs) nanocomposites is heterogeneous and spherical with an average diameter of around 16–30 nm. It is a common knowledge that the morphologies of nanocomposites significantly influenced their adsorption capacity. Adsorbents exhibited a remarkable high adsorption capacity for the removal of methyl orange (MO) from water within a short time interval of 5 min and easy separation of adsorbents after successful adsorption process was achieved with the help of a magnet.	[129]
Polystyrene-thermoplastic	MgAl-LDH	Solution blending technique	The structural morphology of PS/LDH observed to be fibrous membranes. LDH-based sorbent showed a 67% adsorption efficiency of Cd^{2+} ion removal, while LDH-PS fibrous sorbents reached 10–15% adsorption efficiencies of Cd^{2+} ion removal based on the concentration of LDH in each of the sorbents. Since PS fibrous-based sorbents are hydrophobic, then the adsorption efficiency removal of Cd^{2+} ion can be attributed to the involvement of LDH-based sorbents which have better ion exchange capability.	[130]
Polyaniline (PANI)-conductive thermoset	Mg/Al Layered Double Hydroxide	Situ oxidative polymerization	A uniform fibrillar nanostructure is observed by SEM. The maximum adsorption efficiency of the PANI/LDHs is strongly affected by the initial solution pH for Cr(VI) wastewater treatment. Therefore, the adsorption efficiency removal of Cr(VI) decreases while the initial solution pH is above 7.0. This is probably due to the fact that the surface charge of PANI/LDHs was negative when pH > 7.0 and weakened electrostatic repulsion forces and significantly reduced adsorption efficiency/removal percentage of Cr(VI) from wastewater.	[131]

3. Properties of Polymer/Other Clays and LDHs Nanocomposites

The intention for the addition of clay minerals to the polymers is to improve the polymer properties and to produce the polymer/clay nanocomposites with desired applications. The key step is to prepare nanocomposites with highly preferred and value-added demand properties, which overcome downsides of polymers while maintaining their intrinsic advantages. Due to the low cost, availability, high aspect ratio as well as desirable nanostructure and interfacial interactions, clays can provide considerable improved properties at very low filler loadings, which help to obtain more useful properties. The nature and properties of constituents as well as preparation methods and conditions affect the final properties of polymer/clay nanocomposites. In this review, various improved properties of polymer/clay nanocomposites as well as the adsorption capacities and removal efficiency of dyes or heavy metal ions in water including morphology are discussed.

3.1. Morphology of Polymer/Other Clays and LDHs Nanocomposites

The morphology of the polymer/layered clay silicate nanocomposites significantly influenced their adsorption capacities and the removal efficiency of dyes or other heavy metal ions in water. The key aspect in nanocomposite structure is the clay–polymer interaction, which affects the dispersion level of clay in polymer matrix. Depending on the dispersion level of layered silicates, the structure can either be separated, intercalated or exfoliated structure [108,132–135]. Surface modification plays also important role in achieving good interaction between polymer and clay which affects the extent of dispersion and improves significantly the adsorption as well as removal of dyes or heavy metal ions from water. Thus, organically modified clay silicates such as montmorillonite (OMMT), kaolinite and LDH are mostly preferred nano reinforcement for proper selection of the functional groups and their abilities of ion-exchange. It is well-known that acid-modified clay resulted in higher rate of dye adsorption, an increased specific surface area and high porosity than in the case of base-modified clay [136].

Highly flame-retardant polymer/deoxyribonucleic acid (DNA)-modified clay nanocomposites were investigated by transmission electron microscopy (TEM) as shown in Figure 13a–f. The dark lines observed in Figure 13a,d are closely related to the layered silicate nanoclays and the light segments are associated to epoxy matrix. Naebe et al. [137] explained that intra-gallery reactions due to interfacial interactions made diffusion of more epoxy monomers within DNA-modified clay possible to enhance clay layers' separation and therefore induced formation of exfoliated structures as seen in Figure 13b. In addition, three individual intercalated ordered structures known as intercalated tactoids could be observed for epoxy nanocomposite at higher contents of clay (Figure 13e).

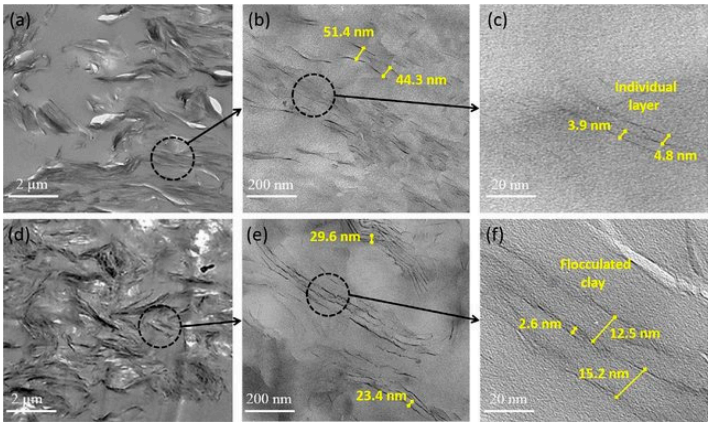

Figure 13. TEM micrographs of epoxy-2.5 wt% of DNA-clay (**a**–**c**) and epoxy-5 wt% of DNA-clay (**d**–**f**) nanocomposites. Reproduced with permission from Reference [137]. Open Access 2016, Springer Nature.

However, few clay layers possess thin and small tactoids which are uniformly and randomly dispersed in the epoxy resin. This indicates that the DNA-clay modification is an effective approach to improve both the exfoliation and dispersion of clay. In addition to achieved dispersion, most of microcracks under an effective load are initiated within the intra-layer of semi-stacked clay instead of epoxy-clay interfacial region. This phenomenon verifies that higher contents of clay (5 wt%) resulted in lower reinforcing impact in the overall mechanical properties.

Evidently, low clay content formed an exfoliated structural configuration with individual layers, well-dispersed with more homogeneous distribution (Figure 13c), while high content of clay resulted in flocculated structures. It can be seen in Figure 13f that phase-separated clay tactoid structures are formed and agglomeration at high content prevail over complete delamination of clay layers due to low penetration of epoxy monomers into stacked layers of modified clay [138].

Zubitur et al. [139] studied the poly(ʟactic acid) (PLA)/modified drug 4-biphenyl acetic acid (Bph)-layered double hydroxide (LDH) nanocomposites. The nanocomposites were prepared by solvent casting with 5 wt% of drug-modified LDH, and the hydrolytic degradation was carried out in a Phosphate-buffered saline (PBS) solution at pH 7.2 and 37.8 °C. From their XRD results, PLA/LDH-Bph nanocomposites showed no peaks corresponding to LDH-Bph observed and this was attributed to an exfoliation or to the presence of entropic LDH layers. The degree of dispersion of acid/base-modified LDH was found to be good with small tactoids at low magnification, exfoliated layers were observed at higher magnification using TEM images. A number of studies reported the acid modification of clay silicate and layered double hydroxides (LDHs) reinforced with polymer matrices. Table 4 represents the summary of selective studies on acid/base-modification of polymer/clay and LDH nanocomposites for water purification.

Table 4. Summary of selective studies on acid/base-modification of polymer/clay and LDH nanocomposites for water purification.

Polymer Systems	Preparation Methods	Acid/Base-Modification	Dispersion and Structural Morphology Good for Removal of Dyes or Heavy Metal Ions.	References.
PLA/ NiAl/LDHs	Melt mixing	SDBS	Good dispersion and predominantly exfoliated structures. Maximum adsorption capacity of dyes or heavy metal ions.	[140]
LDH/PEG_{400}	Physicochemical modification	PEG_{400}	Good dispersion and LDH layers were exfoliated in PEG_{400} and showed higher dye adsorption capacity and effectively removed the azo dye, Acid Orange II (AO-II) in aqueous medium.	[141]
Polyethersulfone (PES)/AA-MMT	Phase inversion method	Acid Activated (AA)	The proper dispersion of nanoparticles in the membrane matrix was observed and PES/AA-MMT showed better dye removal in the basic pH for MO and acidic pH for MB. The nanocomposite membranes exhibited considerably higher dye removal than neat PES. When the nano-clay content was increased, the dye removal percentage also increased in both dyes even in neutral pH due to the remarkable role of MMT particles in dye adsorption.	[142]
Ppy NF/Zn-Fe LDH	Interfacial polymerization of pyrrole	HCl as oxidant	The dispersion was observed to be weak, and structural morphology was separated grain or agglomerated particles-like stacked structure. Ppy NF/Zn-Fe LDH) composites enhanced adsorption capacity and high efficiency in the removal of safranin dye from raw water samples including tap water, groundwater, and sewage water.	[143]
Chitosan (CS)/laponite	Acid Activated (AA) aqueous solution	2-acrylamido-2-methyl-propanesulfonic acid (AMPS)	The degree of dispersion is better after being pre-adsorbed by AMPS and exfoliated microstructure morphology with high surface area, large pore volume and average pore size is observed. High surface area and large amount of micropores in adsorbent is suitable for the penetration of water and heavy metal ions into the interior and thus enhances the adsorption rate and removal efficiency. Thus, these nanocomposites showed an excellent adsorption capacity for removal of Cd(II), MB and CR from aqueous solution rapidly and efficiently.	[144]
Zeo/PVA/SA	Melt blending	The mixture of glutaraldehyde (GA) the cross-linking agent consists of 75 wt% (2% GA, 2% HCl and 71% acetone): 25 wt% DI water.	Zeo/PVA/SA NC beads have more pores and showed rougher and loose surfaces with porous structure. The dispersion of Zeo NPs had some agglomerations and exhibited an irregular inner morphology with stacks of tiny interspace structure with a very limited number of dents. The results revealed the removal efficiency of heavy metal ions such as Pb^{2+}, Cd^{2+}, Sr^{2+}, Cu^{2+}, Zn^{2+}, Ni^{2+}, Mn^{2+} and Li^{2+} using Zeo/PVA/SA NC modified beads reached the maximum at the pH value of 6.0, while the highest removal is achieved at pH = 5 for Fe^{3+} and Al^{3+} with 96.5 and 94.9%, respectively.	[145]
Chitosan/modified Bijoypur clay	Solution blending	HCl-purifier; Dodecylamine	The morphology of modified clay/chitosan showed smooth but discrete spherical particles with some dispersion. Chitosan/modified clay composite with high clay loading showed a better performance for cationic dye (MB) uptake, whereas heavy metals (Cr (VI) and Pb (II)) were better adsorbed on the composite, with high chitosan content.	[146]

3.2. Adsorption of Polymer/Nanoclay and LDH Systems

Various types of polymer/nanoclay composites are currently being explored for the primary usage in water purification and many other applications due to their unique properties, which are different from their counterparts. Polymer/clay nanocomposites used in water purifications technology and their corresponding applications as well as the removal of various heavy metal ions are shown in Figure 14. Adsorption is a removal of soluble material/adsorbed materials called adsorbate (heavy metal ions) present in water and clay nanomaterials (solid adsorbents) are used for the adsorption of contaminants. This process can either be physical (physisorption) or chemical (chemisorption) in nature. Nanoclay minerals have the high specific surface area and high sorption capacity giving high structural and chemical stability towards the adsorption of organic and inorganic contaminants.

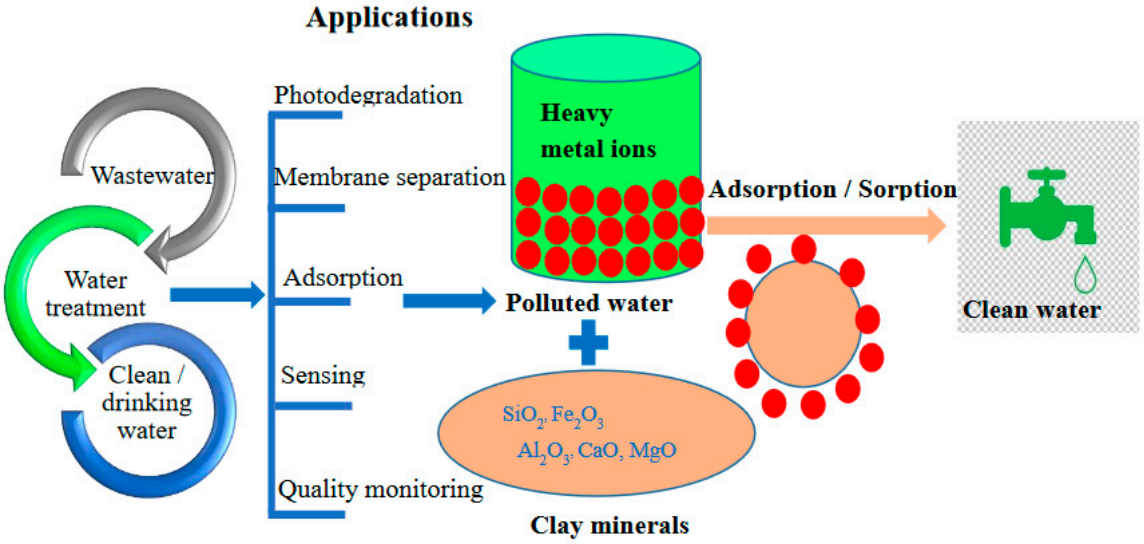

Figure 14. Role of nanocomposite in water purification and the removal of various heavy metal ions.

Due to its high internal surface area in the range of 500–1500 m^2/g, the most popular solid adsorbent material is activated carbon which is primarily used in large-industrial scale for water purification systems [41,49]. Thus, adsorption is a surface phenomenon commonly found in nature and plays a key role in water purification technology. Adsorption increases with the increase in the surface area of the adsorbent. This implies that more finely divided or rougher the surface of the adsorbent is, then the greater is the surface area and the adsorption. However, adsorption affinity of the surface area of the adsorbent is independent of the surface area and dependent on the favorable attractive interactions present at the pH value range below 7. When the pH is higher than 7, the electrostatic repulsion forces of the adsorbate-adsorbent are weakened, hence, the reduced adsorption efficiency or removal percentage of contaminants [41,49,131]. The adsorption of contaminants from water mostly depends on hydrophobic interactions between adsorbate and adsorbent, which make great contributions to the affinity of the organic anion to LDH. Therefore, the hydrophobic interactions interconnect many segments into a cluster in order for each natural organic anion to show a stronger affinity to LDH. The high hydrophilic nature of contaminants reduced significantly the adsorption capacity. The main reason for this is dominant force that decreases the surface tension between the matrix (adsorbent) and the solid adsorbed (adsorbate). The detailed discussion of the effect of pH as one of many factors affecting the adsorption, advantages and disadvantages of various methods of synthesis would also be outlined in the paragraphs or Table 5 below.

Table 5. Advantages and disadvantages of different methods of LDHs and clays in water purification.

Methods	Advantages	Disadvantages	References
Co-precipitation	Has high contaminant removal ability, applicable to communities and low reaction temperature and short reaction time.	Requires high maintenance and optimization of treatment is difficult.	[57,59,61]
Ion exchange	Able to effectively remove inorganic contaminants, has capacity to regenerate and inexpensive. No loss of sorbent on regeneration, effective.	It has high operating costs over a long period of time and cannot effectively remove pyrogens or bacteria. Causes economic limitations, not effective for dispersing and removing the dyes.	[62]
Sonochemical	Produces a better shear thickening transition at lower shear rate and significantly reduced the water content contamination. Improves reaction rate, involves high energies and pressures in a short time; no additives needed; reduced number of reaction steps.	Reactions need to be at certain temperature and there is not enough power to carry out the reaction. Extension of problems; inefficient energy; low yield.	[61,65–67]
Hydrothermal /Solvothermal	Has ability to synthesize large crystals of high quality and crystalline substances that are unstable near the melting point.	High cost of equipment.	[68,69]
Adsorption	The most effective adsorbent, great capacity, produce a high-quality treated effluent.	Ineffective against disperse and dyes, the regeneration is expensive and results in loss of the adsorbent, non-destructive process.	[58,72–75]
Sol–gel method	Can produce a thin coating to ensure excellent adhesion between the substrate and the top layer. It has the capacity of sintering at low temperatures, between 200–600 °C; simple, economical and efficient method to produce high quality coverage and high purity products.	The contraction that occurs during processing; long processing time; fine pores; use of organic solutions that can be toxic.	[76,77]
Urea/Induced hydrolysis	Cheap, easy to store.	Loss through leaching and volatilization, acidifying.	[57,59,60]
In situ polymerization	Easy processing method based on the dispersion of the filler in the polymer precursors.	Difficult control of intragallery polymerization and limited applications.	[18,31,98]
Melt mixing method	One step technique, economical and environmentally viable and easy to process and compatible with industrial polymer processes.	Sensitivity to reaction conditions, limited applications to low molecular weight polymers.	[102–104]
Solution mixing technique	Preparation of homogeneous dispersion of fillers.	The industries and sectors use a huge amount of solvents and this technique is very expensive.	[105,106]

In recent times, different synthesis and preparation methods of LDHs and other nanoclays have been applied as discussed in Sections 2.3 and 2.4, respectively. These different methods influence the adsorption performance of the nanocomposite and noticeably assist to reduce and remove the high concentration levels of contamination in water [147,148]. Individually, each method has some advantages and disadvantages as represented in Table 5. Amongst all the methods, adsorption is considered the most efficient, economical technique and easy processing to drive for contaminants removal from wastewater. Furthermore, the adsorption is reversible, and adsorbents can be regenerated. In general, there are three types of adsorption known as physisorption (the interaction between adsorbent-adsorbate), chemisorption (adsorbent-solvent) and electrostatic interactions (adsorbate-solvent) [149]. The underpinning principles/mechanisms involved in the adsorption material surface have been studied and reported in relation to factors affecting systems.

3.2.1. Factors Governing the Performance of Clays/LDH Based Adsorbents

In this review, the application of nanomaterials as adsorbents for removal of contaminants such as heavy metal ions and dyes from wastewater has been reviewed. It is important to understand how adsorbents interact with different adsorbates such as heavy metal ions and dyes in the laboratory small scale to determine their potential for application in water purification and their contribution to large scale [148,149]. However, the main challenges for adsorption process are waste products, non-selectivity, instability and low/poor heat transfer leading to long heating and cooling times. To address these challenges, the development and design of suitable and more effective nanoadsorbents with optimum adsorption efficiency for the removal of contaminants in water should be prioritized. In the field of wastewater treatment, different materials prepared through various methods bring about unique functionalities for adsorption efficiency for the removal of contaminants from industrial effluents, surface water, groundwater and tap/drinking water. As stated, many key factors affect the efficiency and performance of LDH/clay adsorbents including pH value, contact time, adsorbent dosage, initial ion concentration, temperature, coexisting ions, and sorption kinetics [148,149]. In this

section, the influence of these factors on adsorption performance and capacity by LDH/clay adsorbents is explained as presented in Table 5.

Influence of pH Value

The pH of an adsorbate-adsorbent solution is most significant aspect for adsorptive removal of contaminants. This affects the type of the surface charge of the adsorbent during water purification by the adsorption technique. It is also the main factor taking care of the type of the surface of the adsorbent, degree of ionization and aqueous adsorbates [149]. The effect of solution pH was studied at different pH values from 3.0 to 11.0, and the results are shown in Figure 15a,b. The pH of solution noticeably changed by the addition of diluted HCl/NaOH. The maximum fluoride adsorptions of 98%, 94% and 91%, respectively for cerium bentonite clay-malic acid chitosan (CeBC-A@CS), lanthanum bentonite clay-malic acid chitosan (LaBC-A@CS) and aluminum bentonite clay-malic acid chitosan (AlBC-A@CS) adsorbents was attained at pH of 3.0. It was also reported that the minimum fluoride adsorption for these three different adsorbents was achieved as 43%, 37% and 35%, respectively at pH of 11. At neutral pH of 7.0, the maximum fluoride adsorption was 84%, 82% and 80% for, respectively. The maximum fluoride adsorption capacity can be attributed to the change in the surface charge of the adsorbent. The pH value at point of zero charge (pHzpc) for the adsorbents is 7.1 [150] as represented in Figure 15b. When the pH of solution was less than pHzpc, the fluoride ions moved towards the positively charged surface of the chitosan composites formed by the protonation of OH^- and carboxylic acid groups leading to the fluoride adsorption onto the surface [151]. At a pH value above the pHzpc, the fluoride adsorption was exceptionally low. This is probably because the composite surfaces were negatively charged due to deprotonation of the hydroxyl groups, ensuring mutual repulsion forces between the fluoride ions and the composite surfaces [152]. It can be observed that cerium bentonite clay-malic acid chitosan (CeBC-A@CS) adsorbent showed a higher fluoride adsorption capacity than lanthanum bentonite clay-malic acid chitosan (LaBC-A@CS) and aluminum bentonite clay-malic acid chitosan (AlBC-A@CS) adsorbents.

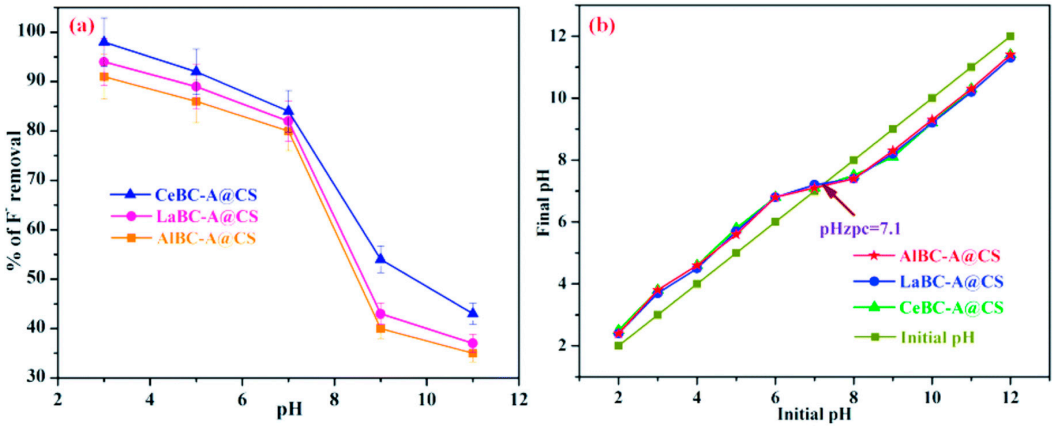

Figure 15. (**a**) Effect of pH and (**b**) pHzpc values of cerium bentonite clay-malic acid chitosan (CeBC-A@CS), lanthanum bentonite clay-malic acid chitosan (LaBC-A@CS) and aluminum bentonite clay-malic acid chitosan (AlBC-A@CS) adsorbents. Reproduced with permission from Reference [151]. Open Access 2020, RSC Advances.

Wei et al. [153] investigated the novel hydrotalcite-like material layered double hydroxide (FeMnMg-LDH) adsorbent synthesized by co-precipitation and its adsorption capacity for the removal of lead ions in water. In order to prevent the precipitation of Pb^{2+} at the high pH, the experiment pH was set below pH 6. The pH of 6 was maintained to prevent the precipitation of Pb^{2+}, and effects of pH on the adsorption are discussed. It was reported that the Pb^{2+} removal percentage by FeMnMg-LDH adsorbent mostly increased with the increasing pH value. The Pb^{2+} removal percentage higher

than 97% at the pH range 3–6, was achieved. This is an indication of the outstanding efficiency and performance of FeMnMg-LDH adsorbent in Pb^{2+} adsorption except when pH is equal to 2. The suspension of the absorbent might take place at extremely low pH resulting into the collapse of the structure of FeMnMg-LDH and therefore reduce Pb^{2+} adsorption efficiency and capability. Comparing the bentonite clay and LDH-based adsorbent, it can be concluded that FeMnMg-LDH adsorbent has a higher adsorption capacity of more 97% than others except the cerium bentonite-malic acid chitosan, which appears to have more or less similar adsorption capacity percentage.

Influence of Contact Time

The contact time significantly affects the adsorption process and the economic efficiency of the process including the adsorption kinetics. Therefore, contact time is profoundly important and dependent factor for performance determination in adsorption process [154]. Figure 16a represents the fluoride adsorption capacity of the three adsorbents (cerium bentonite clay-malic acid chitosan (CeBC-A@CS), lanthanum bentonite clay-malic acid chitosan (LaBC-A@CS) and aluminum bentonite clay-malic acid chitosan (AlBC-A@CS)) at different contact times in the range of 10 to 90 min with neutral pH and initial concentration. The fluoride adsorption capacity of the adsorbents was gradually increased with an increase in contact time. Cerium bentonite clay-malic acid chitosan (CeBC-A@CS) adsorbent obtained the higher fluoride adsorption capacity of 84% than other adsorbents with 62%, 67%, 80%, 82%). Moreover, an equilibrium at 60 min and 45 min was achieved with different adsorbents which suggests the surfaces of the adsorbents CS and BC were completely covered with fluoride ions.

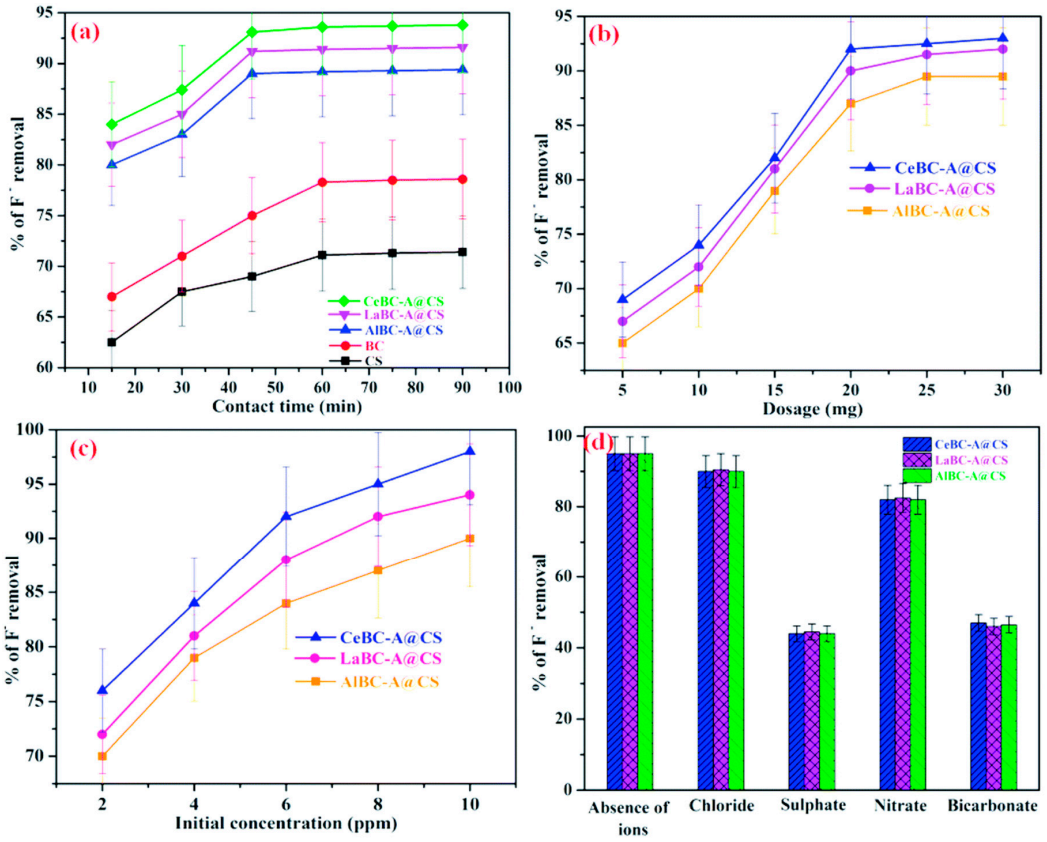

Figure 16. (**a**) Effect of contact time, (**b**) effect of dosage, (**c**) effect of initial fluoride concentration and (**d**) effect of co-ions on the fluoride adsorption of the adsorbents AlBC-A@CS, LaBC-A@CS and CeBC-A@CS at 303 K in neutral pH. Reproduced with permission from Reference [151]. Open Access 2020, RSC Advances.

Jaiswal and Chattopadhyaya [155] studied the effect of contact time on adsorption of Pb(II) on the Co/Bi-LDH synthesized by using co-precipitation method. Their impressive finding was that 90.0% of the adsorptive removal of contaminant, called heavy metal, was accomplished within 120 min of contact time. It was also observed that beyond 120 min, contact time has no effect in heavy metal removal percentage. At the beginning, very high adsorption rates were observed simply because of the larger number of vacancy sites available for the sorption and adsorption equilibria that were then steadily reached [139]. Effect of contact time for bentonite clay and LDH adsorbents using the same co-precipitation method were compared, and it can be concluded that LDH adsorbent seems to have an upper hand in terms of the adsorption capacity percentage for removal of contaminants. The reason for this is that LDH adsorbent has higher surface charge density and more ion exchange binding sites for good adsorption. This could also be attributed to the adsorption on the LDH layers via hydroxide precipitation or metal complexation.

Influence of Adsorbent Dosage

As matter of principle, the degree of adsorption of a solute increase with the increase in the content of an adsorbent. This can be attributed to the increase in adsorbent dosage, which indicates the increased active exchangeable adsorption surface vacancy sites. Nevertheless, the total solute adsorption per unit weight of an adsorbent can decline subsequent to the upsurge in adsorbent dosage because of meddling initiated by the interaction of active sites of an adsorbent [156]. In Figure 16b, the results showed the most favorable dose achieved as 25 mg for the adsorption of fluoride ions via three bentonite clay-based adsorbents. The resultant adsorption capacities of 87%, 90% and 92% were reported for aluminum bentonite clay-malic acid chitosan (AlBC-A@CS), lanthanum bentonite clay-malic acid chitosan (LaBC-A@CS) and cerium bentonite clay-malic acid chitosan (CeBC-A@CS) adsorbents, respectively. Beyond 25 mg, the results showed no significant increase in the fluoride removal limit due to the lower availability of active adsorption sites [157].

Li and co-authors [158] studied Mg–Al layered double hydroxides/MnO_2(Mg–Al LDHs/MnO_2) adsorbents for removal of Pb(II) from aqueous solutions synthesized by one-pot hydrothermal method. It was reported that the adsorbent dosage of Mg–Al LDHs/MnO_2 considerably influenced the adsorptive removal of contaminants like lead ions. It was also observed that the percentage adsorptive removal of Pb(II) contaminant increased fivefold from 18.48% to 99.56% with the adsorbent dosage increasing by a factor of 9 from 0.01 to 0.09 g. In addition, the higher adsorbent dose results in a reduced adsorption capacity of Mg–Al LDHs/MnO_2 at Pb(II) concentration of 50 mg/L. This observation can probably be associated with the low adsorbent dosage leading to the dispersion of Mg–Al LDHs/MnO_2 particles in aqueous solutions. The maximum adsorption efficiency and performance of LDH-based adsorbent and bentonite clay-based adsorbent was achieved at 99.56% and 92%, respectively. The LDH-based adsorbent achieved higher percentage removal efficiency of Pb(II) contaminant than bentonite clay-based adsorbent. This is attributed to the increase in the concentration of adsorption sites in aqueous solution, which enables the contaminants adsorption on a larger number of actives sites.

Influence of Initial Ion Concentration

The influence of the initial ion concentration of the contaminant on the adsorption is one of the most important factors to be studied. It can be seen from Figure 16c that the adsorption capacity of fluoride ions increased with increase in initial concentration. The initial concentrations improved from 2.0 mg per liter to 10 mg per liter where the adsorption capacity/proficiency of the aluminum bentonite clay-malic acid chitosan (AlBC-A@CS), lanthanum bentonite clay-malic acid chitosan (LaBC-A@CS) and cerium bentonite clay-malic acid chitosan (CeBC-A@CS) adsorbents moved from 70.1% to 98% [151]. Thus, the adsorption limit was observed to be straight forward undertaking related to the adsorption of fluoride ions. Mostafa et al. [159] investigated the effect of different Fe(II) concentrations on adsorption capacity of Co/Mo-LDH with carbonate $(CO3)^{2-}$ as an interlayer anion prepared through co-precipitation method. Their results revealed that the Co/Mo-LDH seemingly removed a significant

amount of Fe(II) contaminant from the aqueous solutions. The maximum adsorption efficiency improved to a 99.74%, and the saturation occurred when no more metal ions could be adsorbed on the surface of Co/Mo-LDH. A high efficiency for ferrous adsorption was obtained through a relatively short period of time up to 60 min at initial concentrations of 1.0, 2.0, 3.0 and 5.0 mg/L. The LDH-based adsorbent has 99.74% higher maximum adsorption capacity than bentonite clay-based adsorbent with 98%.

Influence of Co-Existing Ions

The adsorptive removal efficiency of contaminant is typically influenced by the presence of co-existing ions in solution leading to competitive adsorption on the adsorbent surface [160]. The influence of various negatively charged anions such as chloride (Cl^-), sulfate (SO_4^{2-}), nitrate (NO_3^-) and bicarbonate (HCO_3^-) ions on the adsorption of fluoride by the three adsorbents (aluminum bentonite clay-malic acid chitosan (AlBC-A@CS), lanthanum bentonite clay-malic acid chitosan (LaBC-A@CS) and cerium bentonite clay-malic acid chitosan (CeBC-A@CS)) was examined in Figure 16d. The findings suggest that the Cl^- and NO_3^- ions did not change the fluoride adsorption efficiency, while the SO_4^{2-} and HCO_3^- ions had an adverse effect. This can be associated with high coulombic repulsion forces in existence, which reduced the mobility of fluoride ions during interaction with the active sites of the adsorbent. The larger degree of interference of the SO_4^{2-} and HCO_3^- ions is due to the arrival of OH^- ions which induced the arrangement of sodium sulfate and sodium bicarbonate increasing the solution pH and thus made possible for these ions to compete with fluoride ions on the surface of the adsorbent [160].

Zhu et al. [161] studied the effect of calcined Mg/Al layered double hydroxides (Mg-Al LDH) as efficient adsorbents for polyhydroxy fullerenes (PHF) prepared by co-precipitation method. Naturally, PHF may co-exist with other inorganic anions, which may affect its adsorption on layered double oxide (LDO). The effect of selected various coexisting anions such as Cl^-, CO_3^{2-}, SO_4^{2-}, and HPO_4^{2-} at approximately pH of 10 was analyzed. Their results proved that Cl^-, CO_3^{2-}, and SO_4^{2-} slightly improved the adsorption of the PHF on LDO. The adsorption capacity of PHF on LDO lessened considerably in the entire concentration range of PHF with the presence of HPO_4^{2-} ions. The increase in PHF concentration implies that the negative effect of HPO_4^{2-} declined noticeably due to the improved competitive effect of PHF. The effect of co-existing anions on the adsorption of LDH adsorbent may influence the surface property of the adsorbents resulting into two effects known as inhibiting effect and synergistic effect. These happen by occupying some of the adsorption vacant sites (an inhibiting effect) and providing additional adsorption sites (a synergistic effect) [161]. This means that the properties of the adsorbates are influenced by promoting the aggregation or dispersion of adsorbates. Ultimately, the co-existing ions may have various effects such as promoting, inhibiting, or no effect at all on the adsorption of adsorbates of the adsorbents.

Influence of Temperature

The effect of temperature is typically one of the factors governing the adsorption efficiency and performance of adsorbents in water purification systems. An increase in temperature with an increase in the adsorption percentage enables the adsorption capacity of clay/LDH-based adsorbents at various temperatures [162]. This is due to the increase in the mobility of contaminants in aqueous solution, which leads to the improvement in the availability of adsorption vacant surface-active sites. Temperature parameter is well-known to have a strong effect on different chemical processes. It affects the adsorption rate by varying the molecular chain interactions and the solubility of the adsorbate. The effect of temperature on the adsorption of Pb(II) on clay/LDH was investigated by Ayawei et al. [162]. It was observed that on increasing the temperature, the percentage removal of metal ions increased (Figure 17). This presented sufficient evidence to conclusively refer to this adsorption process as an endothermic kind of the process.

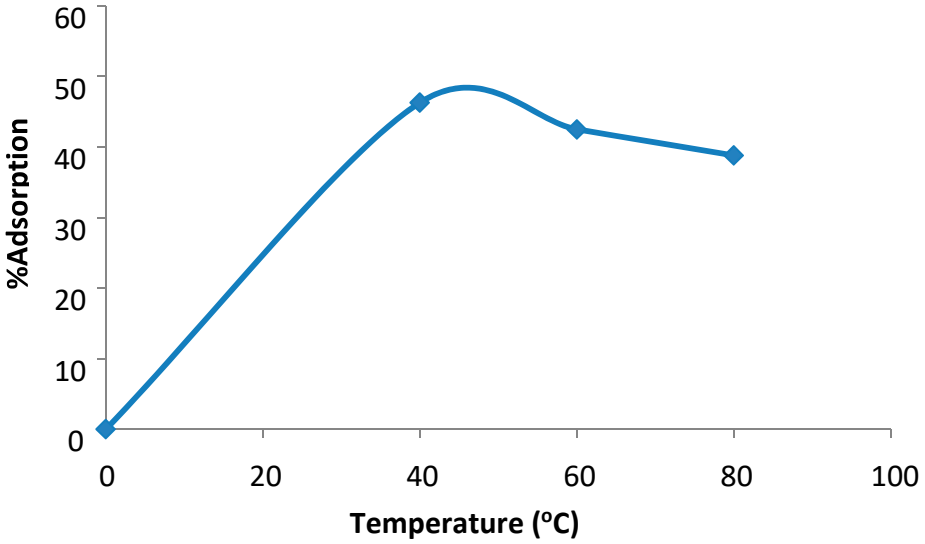

Figure 17. Adsorption capacity and percentage as a function temperature. Reproduced with permission from Reference [162]. Open Access 2015, International Journal of Chemistry.

Influence of Sorption Kinetics and Isotherms

The information on adsorption/desorption process and isotherms is one of the key factors required for proper analysis, structure and understanding of the adsorbent–adsorbate system [160]. In recent times, various models have been explored to explicitly explain the adsorption behavior including isotherm models. The latter provide valuable information about adsorption property of a system and the distribution of exchangeable sites on the surface of the adsorbent. In general sorption, diffusion, desorption, sorption isotherms will be discussed in this section [163].

Some of the factors that play a major role in the adsorption/sorption process are explained below. The nanocomposites usually exhibit a very high amount of barrier properties with even a small amount of layered silicate [29]. Some small molecules such as oxygen, carbon dioxide, water and nitrogen permeate through a polymer membrane due to a gas chemical potential gradient through the membrane. The chemical potential difference ($\Delta\mu$) acts as the driving force for the molecules to permeate from the high chemical potential side to the side of low chemical potential. The mode occurrence of permeant transport in polymers is described using the solution–diffusion model. According to this model, the permeation in polymers consists of three steps as illustrated in Figure 18a (i) sorption of the permeant from the high concentration side onto the membrane/film surface, (ii) diffusion of the permeant along the concentration gradient through the membrane and (iii) desorption through evaporation from the low concentration surface of the membrane. When the permeating molecule interacts with the polymer, then the deviations from a gradient with a straight line can be observed and is known as non-Fickian diffusion explained by the diffusion–relaxation model [164,165].

In this review, we discuss the tortuosity of the diffusive path for nanoplatelets for the gas barrier properties of nanocomposites in Figure 18b. Layered silicate nanoclays such as montmorillonite and kaolinite are the most innovative and promising nanofillers due to their ability to exfoliate to form single nanoplatelets when dispersed in a polymer matrix. The basic theory of the model is that the presence of impermeable clay platelets forces the permeant (gas) molecules to follow a longer diffusion path by traversing around the platelets. Therefore, this is also known as the tortuous path model as illustrated in Figure 18b. The nanoplatelets hinder the diffusion process of small gases through them and form a tortuous path which act as a barrier structure for gases. Tortuous paths explicitly explain the principle of the barrier behavior and its noticeable improvement in nanocomposites, which can be attributed to the impermeability of the layered clay silicate into the polymer matrix. Therefore, the intercalation

molecules are placed in a wiggle shape around the nanoparticles in a random way [166,167] as seen in Figure 18b.

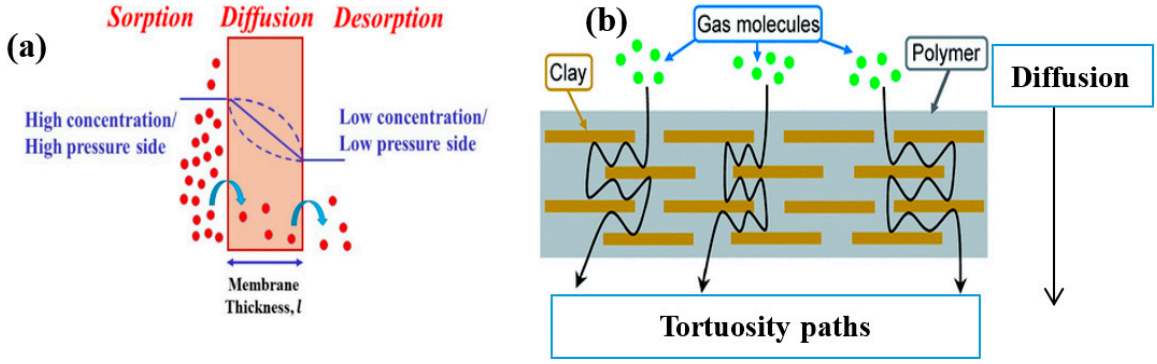

Figure 18. (**a**) Schematic illustration of the solution diffusion model. Reproduced with permission from Reference [168]. Open Access 2020, MDPI Polymers. (**b**) Schematic illustration of the tortuous path model. Reproduced with permission from Reference [95]. Open Access 2017, RSC Advances.

Follain et al. [169] investigated the water vapor transport properties by pervaporation and sorption measurements and evaluated nanoclay extent of dispersion in polymer matrix. They prepared nanocomposites based on poly(ethylene-co-vinyl acetate) (EVA)/organo-modified Cloisite clays at varying contents by melt blending. Their results showed a noticeable decrease in water permeation flux obtained when nanoplatelets are incorporated into the neat EVA matrix (Figure 19a). This barrier effect is typically attributed to the remarkable increase of the diffusion pathways due to organo-modified Cloisite clay-induced tortuosity effects. Furthermore, the water permeation flux seems to be proportional to the diffusion coefficient, which was found to be reduced due to a plasticization effect of water. The water-induced plasticization effect of sorbed water molecules was highlighted through sorption kinetics, and water barrier behavior was observed.

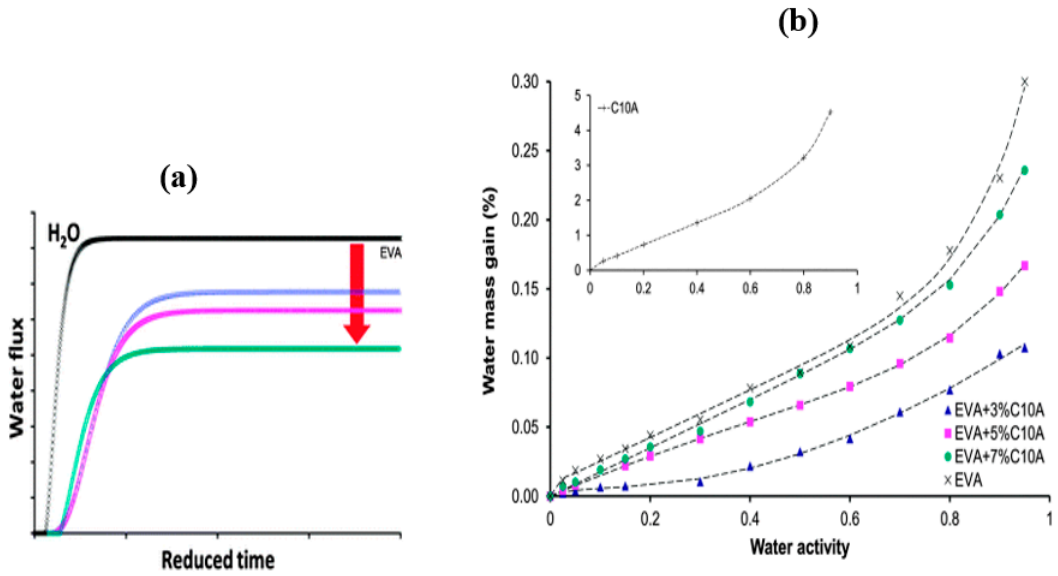

Figure 19. (**a**) Water permeation flux as a function reduced time. (**b**) Water vapor sorption isotherms of the neat EVA matrix and its nanocomposites with an inset of C10A nanoclay isotherm. The dotted lines correspond to the fitting of experimental data with Park's model. Reproduced with permission from Reference [169]. Open Access 2015, The Royal Society of Chemistry.

The water vapor sorption isotherm curves are also known as water mass gain in the equilibrium state versus water activity deduced from water sorption kinetics, reported in Figure 19b. The water sorption capacity of nanoclays is evidently higher than that of the EVA matrix. The incorporation of Cloisite (C10A) into the EVA matrix induced the shift of isotherm curves to lower values at a given activity (Figure 19b), reproducing a reduction in water mass gain. As a result, C10A sorbed higher water mass gain than the matrix, which contributed to increasing sorption capacity of nanocomposites, and this finding is in good agreement with the reduction of water permeability. The decrease in mass gain can be related to tortuosity effects induced by nanoclays in a matrix and which counterbalance the strong water sorption capacity of nanofillers [170]. An increase in nanoclay content, reproduced an increase in water mass gain for nanocomposite samples, which is measured for the whole water activity range due to a more hydrophilic character of nanoclays than the matrix one. This can be attributed to the increase of the polar site number of surfactant-modified nanoclays. The sorption process of the resulting nanocomposites is thus driven by the nanoclay sorption capacity, and the incorporation of nanoclay content into the nonpolar matrix. The nanocomposite with the highest nanoclay loading is categorized by the highest water mass gain. Water molecules are implicitly located in the matrix/nanoclay interfacial regions, and the conclusion is water absorption behavior of nanocomposites obeyed Fick's law. The increased tortuosity within the EVA matrix/nanoclays is therefore in opposite effect to the increased water solubility due to the hydrophilic character of nanoclays.

Rajan et al. [171] studied the role of dicarboxylic acid (malic acid (A)) in chitosan (CS)/modified-metal ion decorated bentonite clay (BC) and the defluoridation efficiency in fluoride contaminated groundwater. The samples were prepared through the solution mixing and their findings revealed the chemical changes of the adsorbent as shown in Figure 20. The bands observed in the range of 3413–3440 cm^{-1} in the spectra of chitosan confirm the presence of O–H bond stretching and N–H bond stretching frequency [172]. The bands at 3046 cm^{-1} and 2900 cm^{-1} related to aliphatic stretching vibrations of –CH, while the bands at 2927 and 2860 cm^{-1} can be attributed to the C–H stretching vibration of the $–CH_2$ groups in chitosan. The aliphatic stretching vibrations of –CH have very low intensity in chitosan [171].

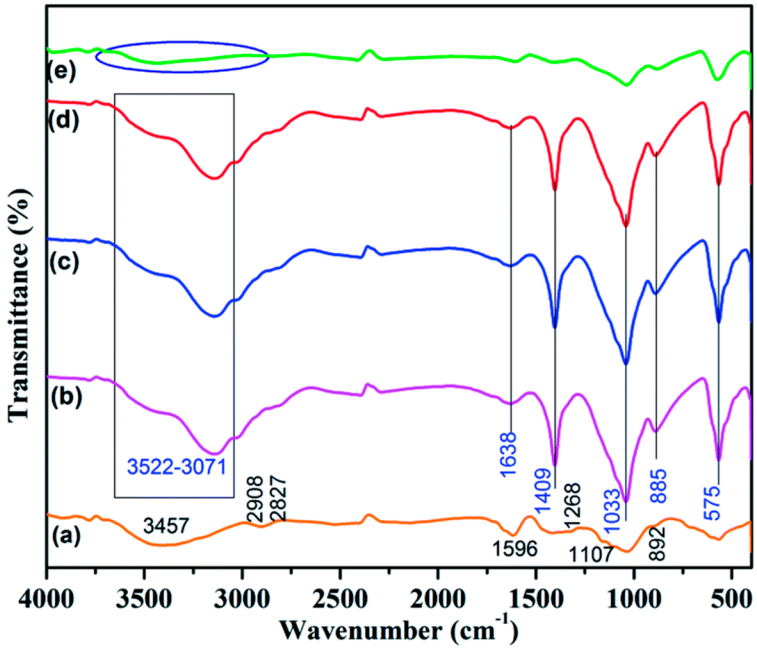

Figure 20. FTIR spectrum of (**a**) chitosan (CS), (**b**) aluminum bentonite clay-malic acid chitosan (AlBC-A@CS), (**c**) LaBC-A@CS, (**d**) cerium bentonite clay-malic acid chitosan (CeBC-A@CS) and (**e**) fluoride adsorbed CeBC-A@CS. Reproduced with permission from Reference [151]. Open Access 2020, RSC Advances.

The peak observed at 1596 cm^{-1} is related to N–H bond scission from the primary amine because of free amino groups in the crosslinked chitosan segments [173]. The peak which appeared at 1596 cm^{-1} indicates the aromatic ring stretching vibration. The C=O adsorption peak of secondary hydroxyl groups becomes more pronounced and shifts to 1107 cm^{-1} [174]. It can be seen in Figure 20e that the peak intensity of the hydroxyl group was remarkably reduced because of the fluoride adsorption. Furthermore, the nitrogen adsorption–desorption analysis was done by Rajan and co-authors [170] as evident in Figure 21. The surface area, pore width and pore volume of the synthesized CeBC-A@CS adsorbent was characterized by Brunauer–Emmett–Teller (BET) analysis and reported as 103 $m^2 \cdot g^{-1}$, 12.71 nm and 0.0321 $cm^3 \cdot g^{-1}$. The synthesized CeBC-A@CS adsorbent possessed high surface area, higher pore width and larger microspore volume, which confirmed that the synthesized adsorbent has maximum adsorption capacity.

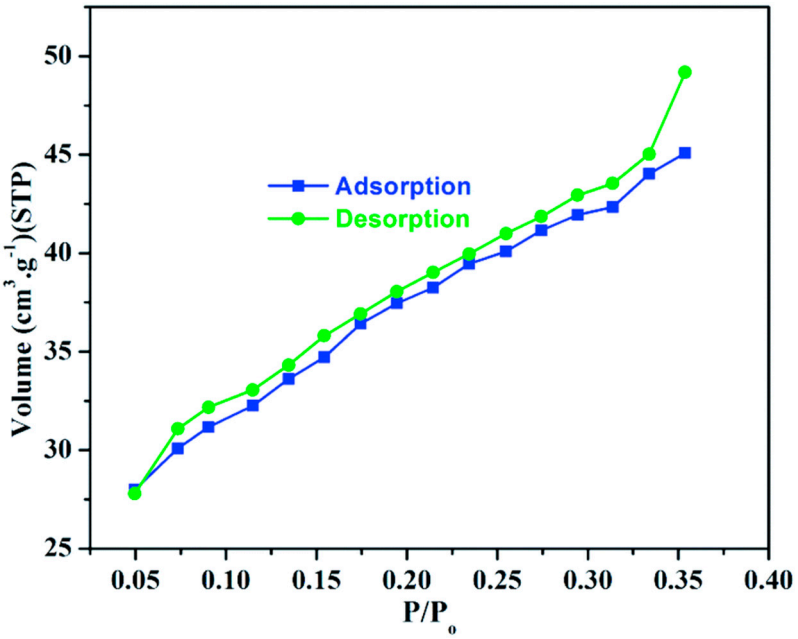

Figure 21. Nitrogen adsorption–desorption isotherm spectrum of cerium bentonite clay-malic acid chitosan (CeBCA@CS) adsorbent. Reproduced with permission from Reference [151]. Open Access 2020, RSC Advances.

4. Concluding Remarks and Future Prospects

In summary, polymer/layered clay nanocomposites are the most progressive and alternative procedures for water purification systems. Synthesis of nanomaterials such as nanoclays and/or LDHs play a pivotal role in improving the physicochemical properties of adsorbents for pollutant removal in water. Furthermore, layered double hydroxides (LDHs) materials have attracted considerable attention and are preferred candidates as sorbents in water treatment because of their remarkable ability to eliminate a variety of water contaminants instantaneously. Their unique properties as anion exchangers and their compositional versatility among other factors is an advantage over other types of clays in the field of water treatment.

Various modification techniques were discussed for the preparation of functionalized clay and LDH nanomaterials and showed influence on the dispersion of nanoclay fillers in the polymer matrices. The desired properties for the polymer/clay and LDH nanocomposites are primarily dependent on the type of modifying agents used for functionalization of layered silicates. Solution blending technique and in situ polymerization method seemed to provide good dispersion of clay layers in polymer matrix compared to melt blending technique. This is mainly because of the low viscosity and high agitation power associated with solution blending. However, melt blending is considered as an industrially

viable as well as ecofriendly technique and shows high economic potential. The addition of stabilizers and/or compatibilizers during the processing stage is believed to lead to an improved number the properties of polymer/clay and LDH nanocomposites.

Development of an appropriate understanding of the structure, property and formulation relationship in both clay-based nanocomposites and LDH based hybrids needs to be further researched for better output in water purification. LDH-containing hybrids are the new emerging areas of research in water purification processes. Due to their nontoxicity, higher surface area than individual constituents and notable adsorption capacity, these LDH hybrids have attracted a considerable interest in water treatment applications. The polymer/modified-clay nanocomposites with exfoliated morphology disclosed strong reduction in water surface tension and efficiently remove methylene blue (MB) dye and other contaminants from water. The adsorption increased with increasing dye concentration, pH values and increasing temperature due to the increased kinetic energies of the molecules. The morphologies of polymer/LDH nanocomposites exhibited a remarkable high adsorption capacity for the efficient removal of dyes and heavy metal ions from water within a short time interval.

Author Contributions: M.M., J.S.S. and M.J.M. conceptualized, co-designed and steered the review as well as co-writing Sections 1, 2, 2.1–2.3 and 3. S.I.M. and K.L. co-wrote Sections 2.4 and 4, while M.M., J.S.S. and M.J.M. compiled the article together. J.S.S. and M.J.M. were responsible for funding acquisition of the manuscript. All authors have read and agreed to the published version of the manuscript.

Funding: This research was funded by the National Research Foundation (NRF) of South Africa, grant number (s) 114270 and 127278.

Acknowledgments: The National Research Foundation (NRF) of South Africa is highly acknowledged for financial support of this research work.

Conflicts of Interest: No conflicts of interest declared by the authors.

Abbreviations

LDHs	Layered double hydroxides	Cl^-	Chloride ion
2D	Two-dimensional	NO^{3-}	Nitrate ion
WHO	World Health Organization	CO_3^{2-}	Carbonate ion
WASH	Water, sanitation and hygiene	N_2	Nitrogen
SDGs	Sustainable development goals	M^{2+}	Divalent cation
MF	Microfiltration	M^{3+}	Trivalent cation
UF	Ultrafiltration	LBL	Layer-by-layer
NF	Nanofiltration	NH_4OH	Ammonium hydroxide
RO	Reverse osmosis	SLNSs	Single layer nanosheets
SMNs	Surface modification of nanomaterials	PVA	Poly(vinyl alcohol)
PCNCs	Polymer clay nanocomposites	PEG	Poly(ethylene glycol)
PNCs	Polymer nanocomposites	HT	Hydrotalcite
MDPI	Multidisciplinary Digital Publishing Institute	PAA	Poly(acrylic acid)
NCs	Nanoclays	POX	Poly(2-oxazoline)
MMT	Montmorillonite	PP	Polypropylene
CEC	Cation exchange capacity	PIP	Polyisoprene
PMMA	Poly(methyl methacrylate)	PLLA	Poly(L-lactic acid)
$Mg(OH)_2$	Magnesium hydroxide	PA11	Polyamide
EVA	Poly(ethylene-co-vinyl acetate)	PAM	Polyacrylamide
$Al(NO_3)_3.9H_2O$	Aluminum nitrate nonahydrate	PE	Polyethylene
$Mg(NO_3)_2.6H_2O$	Magnesium nitrate hexahydrate	PLA	Poly(lactic acid)
BPF	Bio-oil phenolic foam	PS	Polystyrene
MBPF	Modified bio-oil phenolic foam	BT	Bentonite
MAPP	Maleic-anhydride-grafted polypropylene	MB	Methylene Blue
TPU	Thermoplastic polyurethane	CCS	Crosslinked chitosan
NBR	Nitrile butadiene rubber	MO	Methyl orange

PBT	Polybutylene terephthalate	PANI	Polyaniline
NIPAM	N-isopropylacrylamide	DNA	Deoxyribonucleic acid
SEM	Scanning electron microscopy	AA	Acid activated
OMMT	Organically modified montmorillonite	PES	Polyethersulfone
TEM	Transmission electron microscopy	AO-II	Acid Orange II
PBS	Phosphate-buffered saline	Ppy	Polypyrrole
SDBS	Sodium dodecylbenzene sulfonate	CS	Chitosan
AMPS	2-acrylsmido-2-methyl-propanesulfonic acid	SA	Sodium alginate
GA	Glutaraldehyde	NaOH	Sodium hydroxide
HCl	Hydrochloric acid	BC	Bentonite clay
CeBC-A@CS	Cerium bentonite clay-malic acid chitosan		
LaBC-A@CS	Lanthanum bentonite clay-malic acid chitosan		
AlBC-A@CS	Aluminum bentonite clay-malic acid chitosan		
pHzpc	pH zero charge	MnO_2	Manganese dioxide
FeMnMg-LDH	Iron Manganese Magnesium-layered double hydroxide		
DI	Deionized	Pb(II)	Lead ion
RSC	The Royal Society of Chemistry	HCO_3^-	Bicarbonate ion
Co/Mo-LDH	Cobalt/Molybdenum-layered double hydroxide		
PHF	Polyhydroxy fullerenes	SO_4^{2-}	Sulphate ion
SBR	Styrene-butadiene rubber	Cl^-	Chloride ion
VE	Vinyl ester	EP	Epoxy
LDO	Layered double oxide	NO_3^-	Nitrate ion
Mg-Al-LDH	Magnesium-Aluminum-layered double hydroxide		
XRD	X-ray Diffractometry	AB	Amido Black
HPO_4^{2-}	Hydrogen phosphate ion	CH_2	Methylene
N-H	Imidogen	C=O	Carbon monoxide
C10A	Cloisite 10A	C-H	Methylene group
$\Delta\mu$	Chemical potential difference		
BET	Brunauer-Emmett-Teller		
NRF	National Research Foundation		

References

1. Briggs, A.M.; Cross, M.J.; Hoy, D.G.; Sanchez-Riera, L.; Blyth, F.M.; Woolf, A.D.; March, L. Musculoskeletal health conditions represent a global threat to healthy aging: A report for the 2015 World Health Organization world report on ageing and health. *Gerontologist* **2016**, *56*, S243–S255. [CrossRef] [PubMed]
2. Ortigara, A.R.C.; Kay, M.; Uhlenbrook, S. A review of the SDG 6 synthesis report 2018 from an education, training, and research perspective. *Water* **2018**, *10*, 1353. [CrossRef]
3. Ait-Kadi, M. Water for development and development for water: Realizing the sustainable development goals (SDGs) vision. *Aquat. Procedia* **2016**, *6*, 106–110. [CrossRef]
4. Le, N.L.; Nunes, S.P. Materials and membrane technologies for water and energy sustainability. *Sustain. Mater. Techno.* **2016**, *7*, 1–28. [CrossRef]
5. Anjum, M.; Miandad, R.; Waqas, M.; Gehany, F.; Barakat, M.A. Remediation of wastewater using various nano-materials. *Arab. J. Chem.* **2019**, *12*, 4897–4919. [CrossRef]
6. Krstić, V.; Urošević, T.; Pešovski, B. A review on adsorbents for treatment of water and wastewaters containing copper ions. *Chem. Eng. Sci.* **2018**, *192*, 273–287. [CrossRef]
7. Warsinger, D.M.; Chakraborty, S.; Tow, E.W.; Plumlee, M.H.; Bellona, C.; Loutatidou, S.; Karimi, L.; Mikelonis, A.M.; Achilli, A.; Ghassemi, A.; et al. A review of polymeric membranes and processes for potable water reuse. *Prog. Polym.* **2018**, *81*, 209–237. [CrossRef]
8. Pandey, N.; Shukla, S.K.; Singh, N.B. Water purification by polymer nanocomposites: An overview. *Nanocomposites* **2017**, *3*, 47–66. [CrossRef]
9. Tlili, I.; Alkanhal, T.A. Nanotechnology for water purification: Electrospun nanofibrous membrane in water and wastewater treatment. *J. Water Reuse Desal.* **2019**, *9*, 232–248. [CrossRef]

10. Yaqoob, A.A.; Parveen, T.; Umar, K.; Mohamad Ibrahim, M.N. Role of nanomaterials in the treatment of wastewater: A review. *Water* **2020**, *12*, 495. [CrossRef]
11. Guerra, F.D.; Attia, M.F.; Whitehead, D.C.; Alexis, F. Nanotechnology for environmental remediation: Materials and applications. *Molecules* **2018**, *23*, 1760. [CrossRef] [PubMed]
12. Selatile, M.K.; Ray, S.S.; Ojijo, V.; Sadiku, R. Recent developments in polymeric electrospun nanofibrous membranes for seawater desalination. *RSC Adv.* **2018**, *8*, 37915–37938. [CrossRef]
13. Liao, Y.; Loh, C.H.; Tian, M.; Wang, R.; Fane, A.G. Progress in electrospun polymeric nanofibrous membranes for water treatment: Fabrication, modification and applications. *Prog. Polym.* **2018**, *77*, 69–94. [CrossRef]
14. Umar, K.; Parveen, T.; Khan, M.A.; Ibrahim, M.N.M.; Ahmad, A.; Rafatullah, M. Degradation of organic pollutants using metal-doped TiO2 photocatalysts under visible light: A comparative study. *Desal. Water Treat.* **2019**, *161*, 275–282. [CrossRef]
15. Tang, K.; Gong, C.; Wang, D. Reduction potential, shadow prices, and pollution costs of agricultural pollutants in China. *Sci. Total Environ.* **2016**, *541*, 42–50. [CrossRef] [PubMed]
16. Richter, K.E.; Ayers, J.M. An approach to predicting sediment microbial fuel cell performance in shallow and deep water. *Res. J. Appl. Sci.* **2018**, *8*, 2628. [CrossRef]
17. Sizmur, T.; Fresno, T.; Akgül, G.; Frost, H.; Moreno-Jiménez, E. Biochar modification to enhance sorption of inorganics from water. *Bioresour. Technol.* **2017**, *246*, 34–47. [CrossRef]
18. Wang, J.; Wang, Z.; Vieira, C.L.; Wolfson, J.M.; Pingtian, G.; Huang, S. Review on the treatment of organic pollutants in water by ultrasonic technology. *Ultrason. Sonochem.* **2019**, *55*, 273–278. [CrossRef]
19. Liu, C.; Hong, T.; Li, H.; Wang, L. From club convergence of per capita industrial pollutant emissions to industrial transfer effects: An empirical study across 285 cities in China. *Energy Policy* **2018**, *121*, 300–313. [CrossRef]
20. Bayoumi, T.A.; Saleh, H.M. Characterization of biological waste stabilized by cement during immersion in aqueous media to develop disposal strategies for phytomediated radioactive waste. *Prog. Nucl. Energy* **2018**, *107*, 83–89. [CrossRef]
21. Ma, H.; Guo, Y.; Qin, Y.; Li, Y.Y. Nutrient recovery technologies integrated with energy recovery by waste biomass anaerobic digestion. *Bioresour. Technol.* **2018**, *269*, 520–531. [CrossRef] [PubMed]
22. Hlongwane, G.N.; Sekoai, P.T.; Meyyappan, M.; Moothi, K. Simultaneous removal of pollutants from water using nanoparticles: A shift from single pollutant control to multiple pollutant control. *Sci. Total Environ.* **2019**, *656*, 808–833. [CrossRef]
23. Rajasulochana, P.; Preethy, V. Comparison on efficiency of various techniques in treatment of waste and sewage water–A comprehensive review. *Res. Effic. Technol.* **2016**, *2*, 175–184. [CrossRef]
24. Jeevanandam, J.; Barhoum, A.; Chan, Y.S.; Dufresne, A.; Danquah, M.K. Review on nanoparticles and nanostructured materials: History, sources, toxicity and regulations. *Beilstein J. Nanotechnol.* **2018**, *9*, 1050–1074. [CrossRef]
25. Palmero, P. Structural ceramic nanocomposites: A review of properties and powders' synthesis methods. *Nanomaterials* **2015**, *5*, 656–696. [CrossRef]
26. Chen, J.; Liu, B.; Gao, X.; Xu, D. A review of the interfacial characteristics of polymer nanocomposites containing carbon nanotubes. *RSC Adv.* **2018**, *8*, 28048–28085. [CrossRef]
27. Kumar, S.; Nehra, M.; Dilbaghi, N.; Tankeshwar, K.; Kim, K.H. Recent advances and remaining challenges for polymeric nanocomposites in healthcare applications. *Prog. Polym. Sci.* **2018**, *80*, 1–38. [CrossRef]
28. Lofrano, G.; Carotenuto, M.; Libralato, G.; Domingos, R.F.; Markus, A.; Dini, L.; Gautam, R.K.; Baldantoni, D.; Rossi, M.; Sharma, S.K.; et al. Polymer functionalized nanocomposites for metals removal from water and wastewater: An overview. *Water Res.* **2016**, *92*, 22–37. [CrossRef] [PubMed]
29. Müller, K.; Bugnicourt, E.; Latorre, M.; Jorda, M.; Echegoyen Sanz, Y.; Lagaron, J.M.; Miesbauer, O.; Bianchin, A.; Hankin, S.; Bölz, U.; et al. Review on the processing and properties of polymer nanocomposites and nanocoatings and their applications in the packaging, automotive and solar energy fields. *Nanomaterials* **2017**, *7*, 74. [CrossRef]
30. Ashraf, M.A.; Peng, W.; Zare, Y.; Rhee, K.Y. Effects of size and aggregation/agglomeration of nanoparticles on the interfacial/interphase properties and tensile strength of polymer nanocomposites. *Nanoscale Res. Lett.* **2018**, *13*, 214. [CrossRef]
31. Guo, F.; Aryana, S.; Han, Y.; Jiao, Y. A review of the synthesis and applications of polymer–nanoclay composites. *Appl. Sci.* **2018**, *8*, 1696. [CrossRef]

32. Crucho, C.I.; Barros, M.T. Polymeric nanoparticles: A study on the preparation variables and characterization methods. *Mater. Sci. Eng. C* **2017**, *80*, 771–784. [CrossRef] [PubMed]
33. Tessema, A.; Zhao, D.; Moll, J.; Xu, S.; Yang, R.; Li, C.; Kumar, S.K.; Kidane, A. Effect of filler loading, geometry, dispersion and temperature on thermal conductivity of polymer nanocomposites. *Polym. Test.* **2017**, *57*, 101–106. [CrossRef]
34. Ghadimi, M.; Zangenehtabar, S.; Homaeigohar, S. An Overview of the water remediation potential of nanomaterials and their ecotoxicological impacts. *Water* **2020**, *12*, 1150. [CrossRef]
35. Nasir, A.; Masood, F.; Yasin, T.; Hameed, A. Progress in polymeric nanocomposite membranes for wastewater treatment: Preparation, properties and applications. *J. Ind. Eng. Chem.* **2019**, *79*, 29–40. [CrossRef]
36. Schaming, D.; Remita, H. Nanotechnology: From the ancient time to nowadays. *Found. Chem.* **2015**, *17*, 187–205. [CrossRef]
37. Usmani, M.A.; Khan, I.; Ahmad, N.; Bhat, A.H.; Sharma, D.K.; Rather, J.A.; Hassan, S.I. Modification of Nanoclay Systems: An Approach to Explore Various Applications. In *Nanoclay Reinforced Polymer Composites*; Springer: Singapore, 2016; pp. 57–83.
38. Uddin, M.K. A review on the adsorption of heavy metals by clay minerals, with special focus on the past decade. *Chem. Eng. J.* **2017**, *308*, 438–462. [CrossRef]
39. Nadziakiewicza, M.; Kehoe, S.; Micek, P. Physico-chemical properties of clay minerals and their use as a health promoting feed additive. *Animals* **2019**, *9*, 714. [CrossRef]
40. Jawaid, M.; Qaiss, A.; Bouhfid, R. *Nanoclay Reinforced Polymer Composites: Nanocomposites and Bionanocomposites*; Springer: Singapore, 2016; p. 391.
41. Awasthi, A.; Jadhao, P.; Kumari, K. Clay nano-adsorbent: Structures, applications and mechanism for water treatment. *SN Appl. Sci.* **2019**, *1*, 1076. [CrossRef]
42. Jlassi, K.; Krupa, I.; Chehimi, M.M. Overview: Clay preparation, properties, modification. In *Clay-Polymer Nanocomposites*; Elsevier: Amsterdam, The Netherlands, 2017; pp. 1–28.
43. Ghadiri, M.; Chrzanowski, W.; Rohanizadeh, R. Biomedical applications of cationic clay minerals. *RSC Adv.* **2015**, *5*, 29467–29481. [CrossRef]
44. Lázaro, B.B. Halloysite and kaolinite: Two clay minerals with geological and technological importance. *J. Acad. Exact Phys. Chem. Nat. Sci. Zaragoza* **2015**, *70*, 7–38.
45. Yu, F.; Deng, H.; Bai, H.; Zhang, Q.; Wang, K.; Chen, F.; Fu, Q. Confine clay in an alternating multilayered structure through injection molding: A simple and efficient route to improve barrier performance of polymeric materials. *ACS Appl. Mater. Inter.* **2015**, *7*, 10178–10189. [CrossRef] [PubMed]
46. Ferrari, P.C.; Araujo, F.F.; Pianaro, S.A. Halloysite nanotubes-polymeric nanocomposites: Characteristics, modifications and controlled drug delivery approaches. *Cerâmica* **2017**, *63*, 423–431. [CrossRef]
47. Yusoh, K.; Kumaran, S.V.; Ismail, F.S. Surface modification of nanoclay for the synthesis of polycaprolactone (PCL)–clay nanocomposite. In *MATEC Web of Conferences*; EDP Sciences: Pahang, Malaysia, 2018; Volume 150, p. 02005.
48. Irshidat, M.R.; Al-Saleh, M.H. Thermal performance and fire resistance of nanoclay modified cementitious materials. *Constr. Build. Mater.* **2018**, *159*, 213–219. [CrossRef]
49. Murugesan, S.; Scheibel, T. Copolymer/Clay Nanocomposites for Biomedical Applications. *Adv. Funct. Mater.* **2020**, *30*, 1908101. [CrossRef]
50. Wang, W.; Wang, A. Nanoscale Clay Minerals for Functional Ecomaterials: Fabrication, Applications, and Future Trends. In *Handbook of Ecomaterials*; Springer: Cham, Germany, 2019; pp. 1–82.
51. Satish, S.; Tharmavaram, M.; Rawtani, D. Halloysite nanotubes as a nature's boon for biomedical applications. *Nanobiomedicine* **2019**, *6*, 1–16. [CrossRef]
52. Gaaz, T.S.; Sulong, A.B.; Kadhum, A.A.H.; Al-Amiery, A.A.; Nassir, M.H.; Jaaz, A.H. The impact of halloysite on the thermo-mechanical properties of polymer composites. *Molecules* **2017**, *22*, 838. [CrossRef]
53. Lazzara, G.; Cavallaro, G.; Panchal, A.; Fakhrullin, R.; Stavitskaya, A.; Vinokurov, V.; Lvov, Y. An assembly of organic-inorganic composites using halloysite clay nanotubes. *Curr. Opin. Colloid Interface Sci.* **2018**, *35*, 42–50. [CrossRef]
54. Ursino, C.; Castro-Muñoz, R.; Drioli, E.; Gzara, L.; Albeirutty, M.H.; Figoli, A. Progress of nanocomposite membranes for water treatment. *Membranes* **2018**, *8*, 18. [CrossRef]
55. Sajid, M.; Basheer, C. Layered double hydroxides: Emerging sorbent materials for analytical extractions. *Trac-Trend Anal. Chem.* **2016**, *75*, 174–182. [CrossRef]

56. Mir, Z.M.; Bastos, A.; Höche, D.; Zheludkevich, M.L. Recent Advances on the Application of Layered Double Hydroxides in Concrete—A Review. *Materials* **2020**, *13*, 1426. [CrossRef] [PubMed]
57. Mohapatra, L.; Parida, K. A review on the recent progress, challenges and perspective of layered double hydroxides as promising photocatalysts. *J. Mater. Chem.* **2016**, *4*, 10744–10766. [CrossRef]
58. Jaśkaniec, S.; Hobbs, C.; Seral-Ascaso, A.; Coelho, J.; Browne, M.P.; Tyndall, D.; Sasaki, T.; Nicolosi, V. Low-temperature synthesis and investigation into the formation mechanism of high quality Ni-Fe layered double hydroxides hexagonal platelets. *Sci. Rep.* **2018**, *8*, 1–8. [CrossRef] [PubMed]
59. Mishra, G.; Dash, B.; Pandey, S. Layered double hydroxides: A brief review from fundamentals to application as evolving biomaterials. *Appl. Clay Sci.* **2018**, *153*, 172–186. [CrossRef]
60. Barahuie, F.; Hussein, M.Z.; Gani, S.A.; Fakurazi, S.; Zainal, Z. Synthesis of protocatechuic acid–zinc/aluminium–layered double hydroxide nanocomposite as ananticancer nanodelivery system. *J. Solid State Chem.* **2015**, *221*, 21–31. [CrossRef]
61. Yu, J.; Wang, Q.; O'Hare, D.; Sun, L. Preparation of two dimensional layered double hydroxide nanosheets and their applications. *Chem. Soc. Rev.* **2017**, *46*, 5950. [CrossRef]
62. He, X.; Qiu, X.; Hu, C.; Liu, Y. Treatment of heavy metal ions in wastewater using layered double hydroxides: A review. *J. Dispers. Sci. Technol.* **2018**, *39*, 792–801. [CrossRef]
63. Sokol, D.; Klemkaite-Ramanauske, K.; Khinsky, A.; Baltakys, K.; Beganskiene, A.; Baltusnikas, A.; Pinkas, J.; Kareiva, A. Reconstruction effects on surface properties of Co/Mg/Al layered double hydroxide. *Mater. Sci.* **2017**, *23*, 144–149. [CrossRef]
64. Abo El-Reesh, G.Y.; Farghali, A.A.; Taha, M.; Mahmoud, R.K. Novel synthesis of Ni/Fe layered double hydroxides using urea and glycerol and their enhanced adsorption behavior for Cr(VI) removal. *Sci. Rep.* **2020**, *10*, 587. [CrossRef]
65. Pahalagedara, M.N.; Samaraweera, M.; Dharmarathna, S.; Kuo, C.H.; Pahalagedara, L.R.; Gascón, J.A.; Suib, S.L. Removal of azo dyes: Intercalation into sonochemically synthesized NiAl layered double hydroxide. *J. Phys. Chem. C* **2014**, *118*, 17801–17809. [CrossRef]
66. Skorb, E.V.; Möhwald, H.; Andreeva, D.V. Effect of cavitation bubble collapse on the modification of solids: Crystallization aspects. *Langmuir* **2016**, *32*, 11072–11085. [CrossRef] [PubMed]
67. Altay, R.; Sadaghiani, A.K.; Sevgen, M.I.; Sisman, A.; Koşsar, A. Numerical and experimental studies on the effect of surface roughness and ultrasonic frequency on bubble dynamics in acoustic cavitation. *Energies* **2020**, *13*, 1126. [CrossRef]
68. Daud, M.; Kamal, M.S.; Shehzad, F.; Al-Harthi, M.A. Graphene/layered double hydroxides nanocomposites: A review of recent progress in synthesis and applications. *Carbon* **2016**, *104*, 241–252. [CrossRef]
69. Zhao, X.; Cao, J.-P.; Zhao, J.; Hu, G.-H.; Dang, Z.-M. A hybrid Mg–Al layered double hydroxide/graphene nanostructure obtained via hydrothermal synthesis. *Chem. Phys. Lett.* **2014**, *605–606*, 77–80. [CrossRef]
70. Liu, W.; Xu, S.; Liang, R.; Wei, M.; Evans, D.G.; Duan, X. In situ synthesis of nitrogen-doped carbon dots in the interlayer region of a layered double hydroxide with tunable quantum yield. *J. Mater. Chem. C* **2017**, *5*, 3536–3541. [CrossRef]
71. Cermelj, K.; Ruengkajorn, K.; Buffet, J.-C.; O'Hare, D. Layered double hydroxide nanosheets via solvothermal delamination. *J. Ener. Chem.* **2019**, *35*, 88–94. [CrossRef]
72. Wang, L.; Shi, C.; Wang, L.; Pan, L.; Zhang, X.; Zou, J.-J. Rational design, synthesis, adsorption principles and applications of metal oxide adsorbents: A review. *Nanoscale* **2020**, *12*, 4790–4815. [CrossRef]
73. Forano, C.; Bruna, F.; Mousty, C.; Prevot, V. Interactions between biological cells and layered double hydroxides: Towards functional materials. *Chem. Rec.* **2018**, *18*, 1–18. [CrossRef]
74. Larocca, N.M.; Filho, R.B.; Pessan, L.A. Influence of layer-by-layer deposition techniques and incorporation of layered double hydroxides (LDH) on the morphology and gas barrier properties of polyelectrolytes multilayer thin films. *Surf. Coat. Technol.* **2018**, *349*, 1–12. [CrossRef]
75. Shao, M.; Zhang, R.; Li, Z.; Wei, M.; Evans, D.G.; Duan, X. Layered double hydroxides toward electrochemical energy storage and conversion: Design, synthesis and applications. *Chem. Commun.* **2015**, *51*, 15880–15893. [CrossRef]
76. Danks, A.E.; Hall, S.R.; Schnepp, Z. The evolution of 'sol–gel' chemistry as a technique for materials synthesis. *Mater. Horiz.* **2016**, *3*, 91–112. [CrossRef]
77. Zhang, Y.; Li, H.; Du, N.; Zhang, R.; Hou, W. Large-scale aqueous synthesis of layered double hydroxide single-layer nanosheets. Colloids and Surfaces A: Physicochem. *Eng. Asp.* **2016**, *501*, 49–54. [CrossRef]

78. Sarma, G.K.; Rashid, M.H. Synthesis of Mg/Al layered double hydroxides for adsorptive removal of fluoride from water: A mechanistic and kinetic study. *J. Chem. Eng.* **2018**, *63*, 2957–2965. [CrossRef]
79. Sajid, M.; Nazal, M.K.; Baig, N.; Osman, A.M. Removal of heavy metals and organic pollutants from water using dendritic polymers based adsorbents: A critical review. *Sep. Purif. Technol.* **2018**, *191*, 400–423. [CrossRef]
80. Maziarz, P.; Matusik, J.; Leiviskä, T. Mg/Al LDH Enhances Sulfate removal and Clarification of AMD Wastewater in Precipitation Processes. *Materials* **2019**, *12*, 2334. [CrossRef]
81. Daud, M.; Hai, A.; Banat, F.; Wazir, M.B.; Habib, M.; Bharath, G.; Al-Harthi, M.A. A review on the recent advances, challenges and future aspect of layered double hydroxides (LDH)–Containing hybrids as promising adsorbents for dyes removal. *J. Mol. Liq.* **2019**, *288*, 110989. [CrossRef]
82. Li, M.; Tian, R.; Yan, D.; Liang, R.; Wei, M.; Evans, D.G.; Duan, X. A luminescent ultrathin film with reversible sensing toward pressure. *ChemComm* **2016**, *52*, 4663–4666. [CrossRef]
83. Asif, M.; Aziz, A.; Azeem, M.; Wang, Z.; Ashraf, G.; Xiao, F.; Chen, X.; Liu, H. A review on electrochemical biosensing platform based on layered double hydroxides for small molecule biomarkers determination. *Adv. Colloid Interface Sci.* **2018**, *262*, 21–38. [CrossRef]
84. Baig, N.; Sajid, M. Applications of layered double hydroxides based electrochemical sensors for determination of environmental pollutants: A review. *Trends Environ. Anal.* **2017**, *16*, 1–15. [CrossRef]
85. Guan, S.; Liang, R.; Li, C.; Yan, D.; Wei, M.; Evans, D.G.; Duan, X. A layered drug nanovehicle toward targeted cancer imaging and therapy. *J. Mater. Chem. B* **2016**, *4*, 1331–1336. [CrossRef]
86. Yan, L.; Gonca, S.; Zhu, G.; Zhang, W.; Chen, X. Layered double hydroxide nanostructures and nanocomposites for biomedical applications. *J. Mater. Chem. B* **2019**, *7*, 5583–5601. [CrossRef] [PubMed]
87. Bastianini, M.; Faffa, C.; Sisani, M.; Petracci, A. Caffeic Acid-layered Double Hydroxide Hybrid: A New Raw Material for Cosmetic Applications. *Cosmetics* **2018**, *5*, 51. [CrossRef]
88. Amberg, N.; Fogarassy, C. Green consumer behavior in the cosmetics market. *Resources* **2019**, *8*, 137. [CrossRef]
89. Caminade, A.M.; Ouali, A.; Laurent, R.; Turrin, C.O.; Majoral, J.P. Coordination chemistry with phosphorus dendrimers. Applications as catalysts, for materials, and in biology. *Coord. Chem. Rev.* **2016**, *308*, 478–497. [CrossRef]
90. Jing, M.; Hou, H.; Banks, C.E.; Yang, Y.; Zhang, Y.; Ji, X. Alternating voltage introduced NiCo double hydroxide layered nanoflakes for an asymmetric supercapacitor. *ACS Appl. Mater. Inter.* **2015**, *7*, 22741–22744. [CrossRef]
91. Mochane, M.J.; Magagula, S.I.; Sefadi, J.S.; Sadiku, E.R.; Mokhena, T.C. Morphology, Thermal Stability, and Flammability Properties of Polymer-Layered Double Hydroxide (LDH) Nanocomposites: A Review. *Crystals* **2020**, *10*, 612. [CrossRef]
92. Salavagione, H.J.; Diez-Pascual, A.M.; Lázaro, E.; Vera, S.; Gomez-Fatou, M.A. Chemical sensors based on polymer composites with carbon nanotubes and graphene: The role of the polymer. *J. Mater. Chem. A* **2014**, *2*, 14289–14328. [CrossRef]
93. Bhattacharya, M. Polymer nanocomposites—A comparison between carbon nanotubes, graphene, and clay as nanofillers. *Materials* **2016**, *9*, 262. [CrossRef]
94. Madhumitha, G.; Fowsiya, J.; Mohana Roopan, S.; Thakur, V.K. Recent advances in starch–clay nanocomposites. *Int. J. Polym. Anal. Charact.* **2018**, *23*, 331–345. [CrossRef]
95. Cui, Y.; Kumar, S.; Kona, B.R.; van Houcke, D. Gas barrier properties of polymer/clay nanocomposites. *RSC Adv.* **2015**, *5*, 63669–63690. [CrossRef]
96. Hammad, S.; Noby, H.; Elkady, M.F.; El-Shazly, A.H. In-situ of polyaniline/polypyrrole copolymer using different techniques. *Mater. Sci. Eng.* **2017**, *290*, 012001. [CrossRef]
97. Unalan, I.U.; Cerri, G.; Marcuzzo, E.; Cozzolino, C.A.; Farris, S. Nanocomposite films and coatings using inorganic nanobuilding blocks (NBB): Current applications and future opportunities in the food packaging sector. *RSC Adv.* **2014**, *4*, 29393–29428. [CrossRef]
98. Abedi, S.; Abdouss, M. A review of clay-supported Ziegler–Natta catalysts for production of polyolefin/clay nanocomposites through in situ polymerization. *Appl. Catal. A Gen.* **2014**, *475*, 386–409. [CrossRef]
99. Reddy, K.R.; El-Zein, A.; Airey, D.W.; Alonso-Marroquin, F.; Schubel, P.; Manalo, A. Self-healing polymers: Synthesis methods and applications. *Nano Struct. Nano Objects* **2020**, *23*, 100500. [CrossRef]

100. Ozkose, U.U.; Altinkok, C.; Yilmaz, O.; Alpturk, O.; Tasdelen, M.A. In-situ preparation of poly (2-ethyl-2-oxazoline)/clay nanocomposites via living cationic ring-opening polymerization. *Eur. Polym. J.* **2017**, *88*, 586–593. [CrossRef]
101. Cruz, S.M.; Viana, J.C. Structure–Properties Relationships in Thermoplastic Polyurethane Elastomer Nanocomposites: Interactions between Polymer Phases and Nanofillers. *Macromol. Mater. Eng.* **2015**, *300*, 1153–1162. [CrossRef]
102. Jafarbeglou, M.; Abdouss, M.; Shoushtari, A.M.; Jafarbeglou, M. Clay nanocomposites as engineered drug delivery systems. *RSC Adv.* **2016**, *6*, 50002–50016. [CrossRef]
103. Zabihi, O.; Ahmadi, M.; Nikafshar, S.; Preyeswary, K.C.; Naebe, M. A technical review on epoxy-clay nanocomposites: Structure, properties, and their applications in fiber reinforced composites. *Compos. B. Eng.* **2018**, *135*, 1–24. [CrossRef]
104. Ercan, N.; Durmus, A.; Kaşgöz, A. Comparing of melt blending and solution mixing methods on the physical properties of thermoplastic polyurethane/organoclay nanocomposite films. *J. Compos. Mater.* **2017**, *30*, 950–970. [CrossRef]
105. Mohd Zaini, N.A.; Ismail, H.; Rusli, A. Short review on sepiolite-filled polymer nanocomposites. *Polym. Plast. Technol. Eng.* **2017**, *56*, 1665–1679. [CrossRef]
106. Saeed, K.; Khan, I. Characterization of clay filled poly (butylene terephthalate) nanocomposites prepared by solution blending. *Polímeros* **2015**, *25*, 591–595. [CrossRef]
107. Luecha, W.; Magaraphan, R. A novel and facile nanoclay aerogel masterbatch toward exfoliated polymer-clay nanocomposites through a melt-mixing process. *Adv. Mater. Sci. Eng.* **2018**, *2018*, 1–14. [CrossRef]
108. Kong, J.; Li, Z.; Cao, Z.; Han, C.; Dong, L. The excellent gas barrier properties and unique mechanical properties of poly (propylene carbonate)/organo-montmorillonite nanocomposites. *Polym. Bull.* **2017**, *74*, 5065–5082. [CrossRef]
109. Fu, S.; Sun, Z.; Huang, P.; Li, Y.; Hu, N. Some basic aspects of polymer nanocomposites: A critical review. *Nano Mater. Sci.* **2019**, *1*, 2–30. [CrossRef]
110. Pesetskii, S.S.; Bogdanovich, S.P.; & Aderikha, V.N. Polymer/clay nanocomposites produced by dispersing layered silicates in thermoplastic melts. In *Polymer Nanocomposites for Advanced Engineering and Military Applications*; IGI Global: Pennsylvania, PA, USA, 2019; pp. 66–94.
111. Bai, C.; Ke, Y.; Hu, X.; Xing, L.; Zhao, Y.; Lu, S.; Lin, Y. Preparation and properties of amphiphilic hydrophobically associative polymer/montmorillonite nanocomposites. *R. Soc. Open Sci.* **2020**, *7*, 200199. [CrossRef]
112. Szadkowski, B.; Marzec, A.; Rybiński, P.; Żukowski, W.; Zaborski, M. Characterization of Ethylene–propylene Composites Filled with Perlite and Vermiculite Minerals: Mechanical, Barrier, and Flammability Properties. *Materials* **2020**, *13*, 585. [CrossRef]
113. Al-Shahrani, A.; Taie, I.; Fihri, A.; Alabedi, G. Polymer-Clay Nanocomposites for Corrosion Protection. In *Current Topics in the Utilization of Clay in Industrial and Medical Applications*; IntechOpen: London, UK, 2018; pp. 61–79.
114. Alvi, M.U.; Zulfiqar, S.; Sarwar, M.I.; Kidwai, A.A. Preparation and properties of nanocomposites derived from aromatic polyamide and surface functionalized nanoclay. *Chem. Eng. Commun.* **2016**, *203*, 242–250. [CrossRef]
115. Chen, H.H.; Thirumavalavan, M.; Lin, F.Y.; Lee, J.F. A facile approach for achieving an effective dual sorption ability of Si/SH/S grafted sodium montmorillonite. *RSC Adv.* **2015**, *5*, 57792–57803. [CrossRef]
116. Haider, S.; Kausar, A.; Muhammad, B. Overview on polystyrene/nanoclay composite: Physical properties and application. *Polym. Plast. Technol. Eng.* **2017**, *56*, 917–931. [CrossRef]
117. Grishina, E.P.; Ramenskaya, L.M.; Kudryakova, N.O.; Vagin, K.V.; Kraev, A.S.; Agafonov, A.V. Composite nanomaterials based on 1-butyl-3-methylimidazolium dicianamide and clays. *J. Mater. Res. Technol.* **2019**, *8*, 4387–4398. [CrossRef]
118. Bischoff, E.; Simon, D.A.; Liberman, S.A.; Mauler, R.S. Adsorption of ionic liquid onto halloysite nanotubes: Thermal and mechanical properties of heterophasic PE-PP copolymer nanocomposites. In *AIP Conference Proceedings*; AIP Publishing LLC: Jeju Island, Korea, 2016; Volume 1713, pp. 1–5.
119. Xu, P.; Yu, Y.; Chang, M.; Chang, J. Preparation and Characterization of Bio-oil Phenolic Foam Reinforced with Montmorillonite. *Polymers* **2019**, *11*, 1471. [CrossRef] [PubMed]

120. Chanra, J.; Budianto, E.; Soegijono, B. Surface modification of montmorillonite by the use of organic cations via conventional ion exchange method. In *IOP Conference Series: Materials Science and Engineering*; IOP Science: Semarang, Indonesia, 2019; Volume 509, p. 012057.
121. Uwa, C.A.; Jamiru, T.; Sadiku, E.R.; Huan, Z.; Mpofu, K. Polypropylene/nanoclay Composite: A solution to refrigerated vehicles. *Procedia Manuf.* **2019**, *35*, 174–180. [CrossRef]
122. Valapa, R.B.; Loganathan, S.; Pugazhenthi, G.; Thomas, S.; Varghese, T.O. An overview of polymer–clay nanocomposites. In *Clay-Polymer Nanocomposites*; Elsevier: Amsterdam, The Netherlands, 2017; pp. 29–81.
123. Moreno-Sader, K.; García-Padilla, A.; Realpe, A.; Acevedo-Morantes, M.; Soares, J.B.P. Removal of Heavy Metal Water Pollutants (Co2+ and Ni2+) Using Polyacrylamide/Sodium Montmorillonite (PAM/Na-MMT) Nanocomposites. *ACS Omega* **2019**, *4*, 10834–10844. [CrossRef]
124. Atta, A.M.; Al-Lohedan, H.A.; ALOthman, Z.A.; Abdel-Khalek, A.A.; Tawfeek, A.M. Characterization of reactive amphiphilic montmorillonite nanogels and its application for removal of toxic cationic dye and heavy metals water pollutants. *J. Ind. Eng. Chem.* **2015**, *31*, 374–384. [CrossRef]
125. Şen, F.; Demirbaş, Ö.; Çalımli, M.H.; Aygün, A.; Alma, M.H.; Nas, M.S. The dye removal from aqueous solution using polymer composite films. *Appl. Water Sci.* **2018**, *8*, 206. [CrossRef]
126. Peng, N.; Hu, D.; Zeng, J.; Li, Y.; Liang, L.; Chang, C. Superabsorbent cellulose−clay nanocomposite hydrogels for highly efficient removal of dye in water. *ACS Sustainable Chem. Eng.* **2016**, *4*, 7217–7224. [CrossRef]
127. Moja, T.N.; Bunekar, N.; Mojaki, S.; Mishra, S.B.; Tsai, T.-Y.; Hwang, S.S.; Mishra, A.K. Polypropylene–Polypropylene-Grafted-Maleic Anhydride–Montmorillonite Clay Nanocomposites for Pb(II) Removal. *J. Inorg. Organomet. Polym. Mater.* **2018**, *28*, 2799–2811. [CrossRef]
128. Liu, Q.; Yang, B.; Zhang, L.; Huang, R. Adsorption of an anionic azo dye by cross-linked chitosan/bentonite composite. *Int. J. Biol. Macromol.* **2015**, *72*, 1129–1135. [CrossRef]
129. Natarajan, S.; Anitha, V.; Gajula, G.P.; Thiagarajan, V. Synthesis and characterization of magnetic superadsorbent Fe_3O_4-PEG-Mg-Al-LDH nanocomposites for ultrahigh removal of organic dyes. *ACS Omega* **2020**, *5*, 3181–3193. [CrossRef]
130. Alnaqbi, M.A.; Samson, J.A.; Greish, Y.E. Electrospun polystyrene/LDH fibrous membranes for the removal of Cd^{2+} ions. *J. Nanomater.* **2020**, *12*, 5045637. [CrossRef]
131. Quispe-Dominguez, R.; Naseem, S.; Leuteritz, A.; Kuehnert, I. Synthesis and characterization of MgAl-DBS LDH/PLA composite by sonication-assisted masterbatch (SAM) melt mixing method. *RSC Adv.* **2019**, *9*, 658. [CrossRef]
132. Devi, K.U.; Ponnamma, D.; Causin, V.; Maria, H.J.; Thomas, S. Enhanced morphology and mechanical characteristics of clay/styrene butadiene rubber nanocomposites. *Appl. Clay Sci.* **2015**, *114*, 568–576. [CrossRef]
133. Sari, M.G.; Ramezanzadeh, B.; Shahbazi, M.; Pakdel, A.S. Influence of nanoclay particles modification by polyester-amide hyperbranched polymer on the corrosion protective performance of the epoxy nanocomposite. *Corros. Sci.* **2015**, *92*, 162–172. [CrossRef]
134. Tsai, T.Y.; Bunekar, N.; Liang, S.W. Effect of Multiorganomodified LiAl-or MgAl-Layered Double Hydroxide on the PMMA Nanocomposites. *Adv. Polym. Technol.* **2018**, *37*, 31–37. [CrossRef]
135. Nagendra, B.; Mohan, K.; Gowd, E.B. Polypropylene/layered double hydroxide (LDH) nanocomposites: Influence of LDH particle size on the crystallization behavior of polypropylene. *ACS Appl. Mater. Inter.* **2015**, *7*, 12399–12410. [CrossRef]
136. Adeyemo, A.A.; Adeoye, I.O.; Bello, O.S. Adsorption of dyes using different types of clay: A review. *Appl. Water Sci.* **2017**, *7*, 543–568. [CrossRef]
137. Zabihi, O.; Ahmadi, M.; Khayyam, H.; Naebe, M. Fish DNA-modified clays: Towards highly flame retardant polymer nanocomposite with improved interfacial and mechanical performance. *Sci. Rep.* **2016**, *6*, 38194. [CrossRef]
138. Bashar, M.; Mertiny, P.; Sundararaj, U. Effect of nanocomposite structures on fracture behavior of epoxy-clay nanocomposites prepared by different dispersion methods. *J. Nanomater.* **2014**, *70*, 1–12. [CrossRef]
139. Oyarzaba, A.; Mugica, A.; Müller, A.J.; Zubitur, M. Hydrolytic degradation of nanocomposites based on poly(L-lactic acid) and layered double hydroxides modified with a model drug. *J. Appl. Polym. Sci.* **2016**, *133*, 43648.

140. Leng, J.; Kang, N.; Wang, D.Y.; Falkenhagen, J.; Thünemann, A.F.; Schönhals, A. Structure–property relationships of nanocomposites based on Polylactide and layered double hydroxides–comparison of MgAl and NiAl LDH as Nanofiller. *Macromol. Chem. Phys.* **2017**, *218*, 1700232. [CrossRef]
141. Mandal, S.; Kalaivanan, S.; Mandal, A.B. Polyethylene glycol-modified layered double hydroxides: Synthesis, characterization, and study on adsorption characteristics for removal of acid orange II from aqueous solution. *ACS Omega* **2019**, *4*, 3745–3754. [CrossRef] [PubMed]
142. Mahmoudian, M.; Balkanloo, P.G.; Nozad, E. A facile method for dye and heavy metal elimination by pH sensitive acid activated montmorillonite/polyethersulfone nanocomposite membrane. *Chin. J. Polym. Sci.* **2018**, *36*, 49–57. [CrossRef]
143. Mohamed, F.; Abukhadra, M.R.; Shaban, M. Removal of safranin dye from water using polypyrrole nanofiber/Zn-Fe layered double hydroxide nanocomposite (Ppy NF/Zn-Fe LDH) of enhanced adsorption and photocatalytic properties. *Sci. Total Environ.* **2018**, *640–641*, 352–363. [CrossRef] [PubMed]
144. Xu, G.; Zhu, Y.; Wang, X.; Wang, S.; Cheng, T.; Ping, R.; Cao, J.; Kaihe, L. Novel chitosan and Laponite based nanocomposite for fast removal of Cd(II), methylene blue and Congo red from aqueous solution. *e-Polymers* **2019**, *19*, 244–256. [CrossRef]
145. Isawi, H. Using Zeolite/Polyvinyl alcohol/sodium alginate nanocomposite beads for removal of some heavy metals from wastewater. *Arab. J. Chem.* **2020**, *13*, 5691–5716. [CrossRef]
146. Biswas, S.; Rashid, T.U.; Debnath, T.; Haque, P.; Rahman, M.M. Application of chitosan-clay biocomposite beads for removal of heavy metal and dye from industrial effluent. *J. Compos. Sci.* **2020**, *4*, 16. [CrossRef]
147. Sharma, S.; Bhattacharya, A. Drinking water contamination and treatment techniques. *Appl. Water Sci.* **2017**, *7*, 1043–1067. [CrossRef]
148. Sarma, G.K.; Sen Gupta, S.; Bhattacharyya, K.G. Nanomaterials as versatile adsorbents for heavy metal ions in water: A review. *Environ. Sci. Pollut. Res.* **2019**, *26*, 6245–6278. [CrossRef]
149. Crini, G.; Lichtfouse, E.; Wilson, L.; Morin-Crini, N. Adsorption-oriented processes using conventional and non-conventional adsorbents for wastewater treatment. In *Green Adsorbents for Pollutant Removal*; Environmental Chemistry for a Sustainable World; Springer Nature: Besançon, France, 2018; pp. 23–71. ISBN 978-3-319-92111-2.
150. Nagaraj, A.; Munusamy, M.A.; Ahmed, M.; Kumar, S.S.; Rajan, M. Hydrothermal synthesis of a mineral-substituted hydroxyapatite nanocomposite material for fluoride removal from drinking water. *New J. Chem.* **2018**, *42*, 12711–12721. [CrossRef]
151. Nagaraj, A.; Pillay, K.; Kumar, S.K.; Rajan, M. Dicarboxylic acid cross-linked metal ion decorated bentonite clay and chitosan for fluoride removal studies. *RSC Adv.* **2020**, *10*, 16791. [CrossRef]
152. Schneckenburger, T.; Riefstahl, J.; Fischer, K. Adsorption of aliphatic polyhydroxy carboxylic acids on gibbsite: pH dependency and importance of adsorbate structure. *Environ. Sci. Eur.* **2018**, *30*, 1. [CrossRef] [PubMed]
153. Zhou, H.; Jiang, Z.; Wei, S. A new hydrotalcite-like absorbent FeMnMg-LDH and its adsorption capacity for Pb2+ ions in water. *Appl. Clay Sci.* **2018**, *153*, 29–37. [CrossRef]
154. Srivastava, V.; Sharma, Y.; Sillanpää, M. Green synthesis of magnesium oxide nanoflower and its application for the removal of divalent metallic species from synthetic wastewater. *Ceram. Int.* **2015**, *41*, 6702–6709. [CrossRef]
155. Jaiswal, A.; Chattopadhyaya, M.C. Synthesis and characterization of novel Co/Bi-layered double hydroxides and their adsorption performance for lead in aqueous solution. *Arab. J. Chem.* **2017**, *10*, S2457–S2463. [CrossRef]
156. Xie, J.; Lin, Y.; Li, C.; Wu, D.; Kong, H. Removal and recovery of phosphate from water by activated aluminum oxide and lanthanum oxide. *Powder Technol.* **2015**, *269*, 351–357. [CrossRef]
157. Rout, T.K.; Verma, R.; Dennis, R.V.; Banerjee, S. Study the removal of fluoride from aqueous medium by using nanocomposites. *J. Encapsulation Adsorpt. Sci.* **2015**, *5*, 38–52. [CrossRef]
158. Bo, L.; Li, Q.; Wang, Y.; Gao, L.; Hu, X.; Yang, J. One-pot hydrothermal synthesis of thrust spherical Mg–Al layered double hydroxides/MnO_2 and adsorption for Pb(II) from aqueous solutions. *J. Environ. Chem. Eng.* **2015**, *3*, 1468–1475. [CrossRef]
159. Mostafa, M.S.; Bakr, A.A.; Eshaq, G.; Kamel, M.M. Novel Co/Mo layered double hydroxide: Synthesis and uptake of Fe(II) from aqueous solutions (Part 1). *Desalin. Water Treat.* **2014**, *56*, 239–247. [CrossRef]
160. Zhang, L.; Zeng, Y.; Cheng, Z. Removal of heavy metal ions using chitosan and modified chitosan: A review. *J. Mol. Liq.* **2016**, *214*, 175–191. [CrossRef]

161. Zhu, Y.; Zhu, R.; Chen, Q.; Laipan, M.; Zhu, J.; Xi, Y.; He, H. Calcined Mg/Al layered double hydroxides as efficient adsorbents for polyhydroxy fullerenes. *Appl. Clay Sci.* **2018**, *151*, 66–72. [CrossRef]
162. Ayawei, N.; Ekubo, A.T.; Wankasi, D.; Dikio, E.D. Synthesis and Application of Layered Double Hydroxide for the removal of Copper in Wastewater. *Int. J. Chem.* **2015**, *7*, 122–132.
163. Zhou, Q.; Zhu, R.; Parker, S.C.; Zhu, J.; He, H.; Molinari, M. Modelling the effects of surfactant loading level on the sorption of organic contaminants on organoclays. *RSC Adv.* **2015**, *5*, 47022. [CrossRef]
164. El Afif, A. Flow and non-Fickian mass transport in immiscible blends of two rheologically different polymers. *Rheol. Acta* **2015**, *54*, 929–940. [CrossRef]
165. Hairch, Y.; El Afif, A. Mesoscopic modeling of mass transport in viscoelastic phase-separated polymeric membranes embedding complex deformable interfaces. *J. Membr. Sci.* **2020**, *596*, 117589. [CrossRef]
166. Akin, O.; Tihminlioglu, F. Effects of organo-modified clay addition and temperature on the water vapor barrier properties of polyhydroxy butyrate homo and copolymer nanocomposite films for packaging applications. *J. Polym. Environ.* **2018**, *26*, 1121–1132. [CrossRef]
167. Barik, S.; Badamali, S.K.; Behera, L.; Jena, P.K. Mg–Al LDH reinforced PMMA nanocomposites: A potential material for packaging industry. *Compos. Interfaces* **2018**, *25*, 369–380. [CrossRef]
168. Singha, S.; Hedenqvist, M.S. A Review on Barrier Properties of Poly (Lactic Acid)/Clay Nanocomposites. *Polymers* **2020**, *12*, 1095. [CrossRef]
169. Wilson, R.; Follain, N.; Tenn, N.; Kumar, A.; Thomas, S.; Marais, S. Tunable water barrier properties of EVA by clay insertion? *Phys. Chem. Chem. Phys.* **2015**, *17*, 19527–19537. [CrossRef]
170. Trifol, J.; Plackett, D.; Szabo, P.; Daugaard, A.E.; Giacinti Baschetti, M. Effect of Crystallinity on Water Vapor Sorption, Diffusion, and Permeation of PLA-Based Nanocomposites. *ACS Omega* **2020**, *5*, 15362–15369. [CrossRef]
171. Smit, W.J.; Tang, F.; Nagata, Y.; Sánchez, M.A.; Hasegawa, T.; Backus, E.H.; Bonn, M.; Bakker, H.J. Observation and identification of a new OH stretch vibrational band at the surface of ice. *J. Phys. Chem. Lett.* **2017**, *8*, 3656–3660. [CrossRef]
172. Lichawska, M.E.; Bodek, K.H.; Jezierska, J.; Kufelnicki, A. Coordinative interaction of microcrystalline chitosan with oxovanadium (IV) ions in aqueous solution. *Chem. Cent. J.* **2014**, *50*, 1–9. [CrossRef] [PubMed]
173. Ivanova, O.P.; Krinichnaya, E.P.; Morozov, P.V.; Zav'yalov, S.A.; Zhuravleva, T.S. The Effect of Filler Content on the IR Spectra of Poly (p-xylylene)–Sulfide Nanocomposites. *Nanotechnol. Russ.* **2019**, *14*, 7–15. [CrossRef]
174. Homaeigohar, S. The nanosized dye adsorbents for water treatment. *Nanomaterials* **2020**, *10*, 295. [CrossRef] [PubMed]